

1  
2  
3  
4  
5  
6  
7  
8  
9  
10  
11  
12  
13  
14  
15  
16  
17  
18  
19  
20  
21  
22  
23  
24  
25  
26  
27  
28  
29  
30  
31  
32  
33  
34  
35  
36  
37  
38  
39  
40  
41  
42  
43

# The RNA chaperone protein CspA stimulates translation during cold acclimation by promoting the progression of the ribosomes

***Anna Maria Giuliadori<sup>1\*</sup>, Riccardo Belardinelli<sup>2,3</sup>, Melodie Duval<sup>2</sup>, Raffaella Garofalo<sup>2</sup>, Emma Schenckbecher<sup>2</sup>, Vasili Hauryliuk<sup>4</sup>, Eric Ennifar<sup>2</sup> and Stefano Marzi<sup>2\*</sup>***

<sup>1</sup>School of Biosciences and Veterinary Medicine, University of Camerino, Camerino, Italy

<sup>2</sup>Université de Strasbourg, CNRS, Architecture et Réactivité de l'ARN, UPR 9002, F-67000 Strasbourg, France

<sup>3</sup>Current address: Department of Physical Biochemistry, Max Planck Inst. for Biophysical Chemistry, Goettingen, Germany

<sup>4</sup>Department of Experimental Medical Science, Lund University, 221 00 Lund, Sweden and University of Tartu, Institute of Technology, 50411 Tartu, Estonia

\*Corresponding authors:

Dr. Stefano MARZI  
UPR 9002 CNRS-ARN  
Université De Strasbourg  
IBMC  
15 Rue René Descartes  
67084 Strasbourg-France  
Phone +33 (0)3 88417051  
Fax: +33 (0)3 88602218  
E-mail: [s.marzi@ibmc-cnrs.unistra.fr](mailto:s.marzi@ibmc-cnrs.unistra.fr)

Dr. Anna Maria Giuliadori  
Laboratory of Genetics of Microorganisms and Microbial Biotechnology  
Department of Biosciences and Veterinary Medicine  
University of Camerino,  
62032 Camerino (MC), Italy  
Phone +39 0737 403206  
Fax +39 0737 636216  
E-mail: [annamaria.giuliadori@unicam.it](mailto:annamaria.giuliadori@unicam.it)

Running title: CspA activity during translation in the cold

44 SUMMARY (174 words)

45  
46 CspA is an RNA binding protein expressed during cold-shock in *Escherichia coli*,  
47 capable of stimulating translation of several mRNAs – including its own – at low  
48 temperature. We used reconstituted translation systems to monitor the effects of CspA on  
49 the different steps of the translation process and probing experiments to analyze the  
50 interactions with its target mRNAs. We specifically focused on *cspA* mRNA which adopts a  
51 cold-induced secondary structure at temperatures below 20°C and a more closed  
52 conformation at 37°C. We show that at low temperature CspA specifically promotes the  
53 translation of the mRNA folded in the conformation less accessible to the ribosome (37°C  
54 form). CspA interacts with its mRNA without inducing large structural rearrangement, does  
55 not bind the ribosomal subunits and is not able to stimulate the formation of the translation  
56 initiation complexes. On the other hand, CspA promotes the progression of the ribosomes  
57 during translation of its mRNA at low temperature and this stimulation is mRNA structure-  
58 dependent. A similar structure-dependent mechanism may be responsible for the CspA-  
59 dependent translation stimulation observed with other probed mRNAs, for which the  
60 transition to the elongation phase is progressively facilitated during cold acclimation with  
61 the accumulation of CspA.

62

## 63 INTRODUCTION

64 Cold is a physical stress that influences conformation, flexibility, topology and  
65 interactions of every macromolecule in the cell. When subjected to abrupt temperature  
66 downshifts, mesophilic bacteria stop growing for several minutes until acclimation is  
67 established and growth resumes at lower temperature (for a review, see Giuliodori, 2016;  
68 Barria et al., 2013; Gualerzi et al., 2003; Weber and Marahiel, 2003). This cold acclimation  
69 phase is accompanied by drastic reprogramming of gene expression: whereas RNA,  
70 protein and lipid synthesis rates are in general reduced, the production of a small set of  
71 cold-shock (CS) proteins transiently increases (Giuliodori, 2016; Gualerzi et al., 2003;  
72 Phadtare and Inouye, 2004). These CS proteins are mainly transcription and translation  
73 factors as well as proteins involved in RNA structure remodeling, such as RNA  
74 chaperones, RNA helicases, and exoribonucleases (Jones et al., 1996; Bae et al., 2000;  
75 Yamanaka and Inouye, 2001; Gualerzi et al., 2003; Cairrão et al., 2003). The induction of  
76 CS gene expression is done at both the transcriptional and post-transcriptional levels  
77 (Gualerzi et al., 2003). Surprisingly, an increase in mRNA abundance after cold-shock  
78 does not necessarily lead to an increased synthesis of the corresponding protein  
79 (Goldenberg et al., 1997). The likely explanation is that low temperature impairs translation,  
80 affecting both the initiation (Broeze et al. 1978; Farewell and Neidhardt, 1998; Zhang et al.,  
81 2018) and the elongation (Friedman and Weinstein, 1964; Farewell and Neidhardt, 1998;  
82 Zhang et al., 2018) phases. The ability of the translational machinery to synthesize  
83 proteins under these unfavorable conditions relies on *cis*-acting elements encoded in  
84 mRNAs, whose existence was demonstrated in cells (Mitta et al., 1997; Yamanaka et al.,  
85 1999; Etchegaray and Inouye, 1999; Zhang et al., 2018) and using *in vitro* assays  
86 (Giuliodori et al., 2010, Giuliodori et al, 2019). *Trans*-acting factors play an important role  
87 in this process, such as the initiation factors IF1 and IF3, and the protein CspA, whose

88 levels specifically increase during cold-shock (Giuliodori et al., 2004; Giuliodori et al.,  
89 2007; Di Pietro et al., 2013; Zhang et al., 2018). The timing of cold-shock gene induction  
90 suggests that the expression of some CS genes might be dependent on the synthesis of  
91 early CS proteins (Weber and Marahiel, 2003; Zhang et al., 2018).

92 CspA, a member of the CS protein (Csp) family, is the most well-studied *E. coli* CS  
93 protein (Yamanaka et al., 1998). Out of the nine paralogues, seven are cold-inducible  
94 (CspA, CspB, CspE, CspF, CspG, CspH and CspI) and two are expressed only at 37°C  
95 (CspC and CspD) (Giuliodori 2016, Zhang et al, 2018). Furthermore, expression of CspF  
96 and CspH is also induced upon urea challenge (Withman et al., 2013). To generate a cold-  
97 sensitive phenotype, four out of the nine *csp* genes must be knocked out in *E. coli* genome,  
98 and this cold-sensitive phenotype can be reverted by overexpressing any of the *csp*  
99 members, with the exception of *cspD* (Xia et al., 2001). CspA is a small protein of 70  
100 amino acids comprised of a single OB fold domain, similar to S1 domain (Newkirk et al.,  
101 1994; Schindelin et al., 1994). The protein preferentially binds single strand regions of  
102 RNA and DNA (Jiang et al, 1997), but the sequence specificity of the interaction is still  
103 unclear. While some reports show preferential binding of CspA to polypyrimidine-rich  
104 sequences (Lopez and Makhatadze, 2000), others studies suggest that CspA lacks  
105 sequence specificity (Jiang et al., 1997). Importantly, the 5'-UTR *cspA* mRNA encoding  
106 CspA was suggested to be a *bona fide* target of CspA-mediated regulation (Jiang et al.  
107 1997). In *E. coli* the extent of cold shock induction of *cspA* mRNA is growth phase-  
108 dependent (Brandi et al., 1999). When cells are subjected to cold-shock during mid-late  
109 exponential growth, they abundantly transcribe and translate *cspA* mRNA *de novo* to  
110 increase the level of the protein. Conversely, when cells are subjected to cold-shock in the  
111 early stage of growth, they use CspA and its transcript synthesized at 37°C predominantly,  
112 at least at the beginning of the cold adaptation phase.

113 While several structures of Csp proteins are available – namely, *E. coli* CspA  
114 (Newkirk et al., 1994; Schindelin et al., 1994), *B. subtilis* CspB (Schindelin et al., 1993;  
115 Schnuchel et al., 1993), *B. caldolyticus* CspB (Mueller et al., 2000), and *Thermotoga*  
116 *maritima* CspB (Kremer et al., 2001) – only two structures of RNA-Csp protein complexes  
117 have been determined. Specifically, the crystal structure of *B. subtilis* CspB – the major  
118 cold shock protein in this bacterium – has been solved in complex with two  
119 oligoribonucleotides: 5'-UUUUUU-3' and 5'-GUCUUUA-3' providing a framework to  
120 explain how the OB fold domain interacts with RNA (Sachs et al., 2012). Seven aromatic  
121 residues and two lysines located on the surface of CspB are the key players in binding to  
122 RNA.

123 Even if the rules governing the CspA-RNA interaction are not known, its low binding  
124 selectivity and affinity (association constant in the  $\mu\text{M}$  range (Jiang et al., 1997; Phadtare  
125 and Inouye, 1999; Lopez and Makhatadze, 2000) are typical of RNA chaperone proteins,  
126 which bind RNAs only transiently (Mayer et al., 2007; Rajkowitsch and Schroeder, 2007;  
127 Duval et al., 2017). However, CspA is a highly abundant protein during cold stress: it  
128 accounts for up to 10% of the total proteins during cold adaptation (Brandi et al., 1999),  
129 with intracellular CspA concentration reaching 100  $\mu\text{M}$  (Bae et al., 1999; Brandi et al.,  
130 1999). Therefore, it is expected that in cold-stressed cells several molecules of CspA could  
131 bind simultaneously to an individual target mRNA (Ermolenko and Makhatadze, 2002;  
132 Zhang et al., 2018). Given CspA propensity to bind single strand (ss) regions in nucleic  
133 acids, the protein is expected to play an important role in modulating mRNA structures  
134 induced/stabilized by low temperatures, thus playing crucial role in regulating their  
135 expression. This hypothesis is supported by experiments showing that (i) CspA promotes  
136 melting of the secondary structure of MS2 mRNA (Phadtare et al., 2009), (ii) CspA acts as  
137 both transcriptional (La Teana et al., 1991; Jones et al., 1992) and translational (Giuliodori

138 et al., 2004) activator in the cold, and (iii) CspA acts as an RNA chaperone (Jiang et al.,  
139 1997; Rennella et al., 2017; Zhang et al., 2018).

140         Several crucial questions regarding the cellular functions of CspA and its mechanism  
141 of action still remain to be answered. As, for example, the determinants for CspA activation  
142 of specific target genes and the mechanism for CspA-dependent stimulation of their  
143 expression. In the present work, we have characterized the mechanism of translational  
144 activation of *cspA* mRNA by CspA using a cell-free reconstituted translation system and  
145 probing methods. The translation efficiency of the two forms of *cspA* mRNA was  
146 compared: the newly synthesized mRNA adopts an open, cold-induced, conformation  
147 below 20°C and a more closed conformation at 37°C, which is stabilized at low  
148 temperatures (Giuliodori et al., 2010). Using the two *cspA* mRNA forms in translation  
149 assays performed at low temperature, we demonstrate that CspA specifically promotes  
150 translation of the mRNA with the more closed structure. Combining crosslinking and  
151 footprinting approaches, we demonstrate that CspA binds to the two *cspA* mRNA  
152 conformations at various positions. However, CspA binding is neither able to unwind the  
153 structures of the stably folded mRNA nor capable of promoting the formation of translation  
154 initiation complexes. Our experiments suggest that at low temperature, CspA assists the  
155 progression of ribosomes along its highly structured mRNA. Furthermore, we demonstrate  
156 by cross-linking experiments that CspA binds to other mRNAs preferentially in a position  
157 located downstream from the initiation codon and can stimulate the translation of some of  
158 the bound transcripts. Indeed, analysis of available ribosome profiling data during cold  
159 acclimation shows that these CspA-dependent mRNAs present ribosomes stalled on the  
160 initiation codons, which progress to translation elongation with the cellular accumulation of  
161 CspA. Eventually, we proposed a model that takes into account these results and explain  
162 the translation activity of CspA upon cold shock.

163

## 164 **RESULTS**

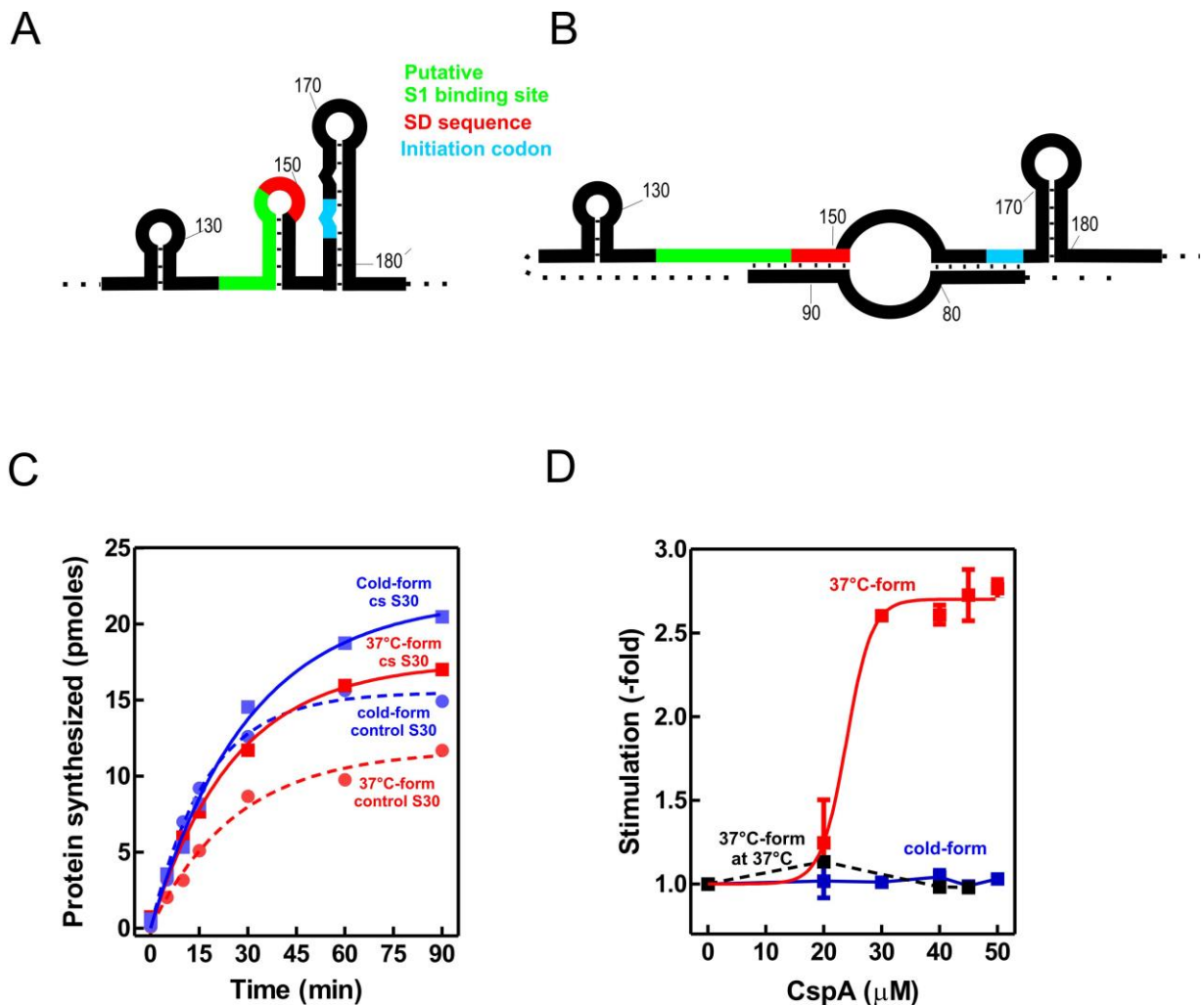
### 165 *CspA favors the translation of less favorable structure of cspA mRNA during cold shock*

166 To uncover the possible effects of cold-shock trans-acting factors on the translation  
167 of mRNAs with unfavorable secondary structures at low temperature, we first used a  
168 translation cell-free system using crude S30 extracts (i.e. a bacterial content deprived from  
169 membrane debris) prepared from cells grown at 37°C (control) or exposed to 15°C for 120  
170 minutes (cs extracts). The latter type of extract contains high levels of cold-shock proteins  
171 synthesized when cells reprogram their genetic expression after sensing the cold  
172 (Giuliodori, 2016). *In vitro* translation reactions were programmed with *cspA* mRNA, which  
173 acts as useful tool for studying structural transitions in RNA and the role of CS factors.  
174 After denaturation at 90°C, this transcript can be refolded in two different structures: the  
175 cold-structure, which exists only at a temperature below 20°C, and the 37°C-structure  
176 (Giuliodori et al., 2010). While the cold-structure is competent in efficient recruitment of  
177 30S ribosomal subunits to AUG initiation codon (Figure 1A), in the 37°C-form both the  
178 Shine-Dalgarno sequence (SD) and the initiation codon are partially occluded (Figure 1B).  
179 Notably, the 37°C-form is very stable and is maintained and stabilized upon incubation at  
180 low temperature (Giuliodori et al., 2010).

181 The translational activities of the two *cspA* mRNA forms were tested with the two  
182 types of cell extracts at 15°C (Fig. 1C). The data show that the cold structure is more  
183 efficiently translated than the 37°C-structure. However, during the first 30 minutes of the  
184 time-course, the extracts from cold-shocked cells translate with similar efficiency both  
185 forms of *cspA* mRNA. This suggests that the intracellular milieu of cold-treated *E. coli* is  
186 enriched in factors that support the translation of the mRNA with the less favorable  
187 secondary structure. Since the most abundant protein in the cold-shock extract – CspA –



188 is able to stimulate protein synthesis at low temperature (Giuliodori et al., 2004), we next  
189 investigated its role in translation. To this end, translation of the cold- and 37°C-forms of  
190 *cspA* mRNA was studied in the presence of increasing amounts of purified CspA using  
191 70S ribosomes and post-ribosomal supernatant (S100) prepared from cells that were not  
192



219 **FIGURE 1. Effect of CspA on *cspA* mRNA translation at low temperature.** Schematic  
220 representation of the secondary structures of the Translation Initiation Region (TIR) of the A) cold-  
221 form and B) 37°C of *cspA* mRNA. The SD sequence, the start codon and the putative S1-binding  
222 site are indicated in red, light blue and green, respectively (Giuliodori et al., 2010). (C) *in vitro*  
223 translation at 15°C with control (dashed lines) and cold-shock (solid lines) S30 extracts; the  
224 experiments were carried out with *cspA* mRNA folded in the cold-form (blue symbols) or in the  
225 37°C-form (red symbols). (D) *in vitro* translation with control 70S and S100 in the presence of the  
226 indicated amounts of purified CspA at 15°C (solid line) with the cold-form (blue) or the 37°C-form  
227 (red) of *cspA* mRNA. The reaction was also performed at 37°C only with the 37°C-form (dashed  
228 black line). Data points in panel B are the average of two independent experiments. Error bars  
229 represent the standard deviations. Further details are given in Materials and Methods.  
230



231 exposed to low temperature (Fig. 1D). The reactions were carried out at 15°C with the two  
232 forms of *cspA*, whereas at 37°C only the activity of the 37°C-structure of *cspA* mRNA  
233 could be probed, as the cold structure exists only at temperatures below 20°C (Giuliodori  
234 et al., 2010). Our results (Fig. 1D) clearly demonstrate that CspA strongly promotes (> 2.5-  
235 fold) the translation of the less-favorable 37°C-structure of *cspA* mRNA at low temperature,  
236 while it does not affect the translation of the other and more open *cspA* mRNA form. The  
237 effect is strongly dose-dependent, as the translation sharply increased when CspA  
238 concentration rises above 20-25 µM. Interestingly, this stimulatory activity of CspA is not  
239 observed at 37°C.

240

241 *CspA assists the progression of the ribosome along the structured mRNA at low*  
242 *temperature*

243 To investigate the mechanism by which CspA stimulates the translation process, we  
244 tested the effect of purified CspA on the recruitment of the mRNA conformers to the 30S  
245 subunit either in the presence (Fig. 2A) or in the absence (Fig. 2B) of IFs and the initiator  
246 fMet-tRNA<sub>i</sub><sup>Met</sup>. We established that CspA does not assist the binding of its mRNA to the  
247 small ribosome subunit, and we confirmed that the cold-form mRNA binds better  
248 (approximately 2.5-fold) to the 30S subunits than the 37°C-form mRNA (Giuliodori et al.,  
249 2010). Next, using filter binding (Fig. 2C) and toeprinting assays (Fig. 2D), we probed the  
250 ability of CspA to promote the binding of fMet-tRNA<sub>i</sub><sup>Met</sup> to the 30S subunits and the  
251 consequent formation of the active initiation complexes in the presence of the 37°C-form of  
252 *cspA* mRNA at low temperature. The two experiments showed that the assembly of the  
253 initiation complex is insensitive to the addition of CspA.

254 We next explored whether this protein could stimulate the translation elongation step  
255 in the cold. To this end, we have developed a test system based on the *E. coli* RelE toxin,  
256 which cleaves between the second and the third nucleotide of the mRNA codon in the

257

258

259

260

261

262

263

264

265

266

267

268

269

270

271

272

273

274

275

276

277

278

279

280

281

282

283

284

285

286

287

288

289

290

291

292

293

294

295

296

297

298

299

300

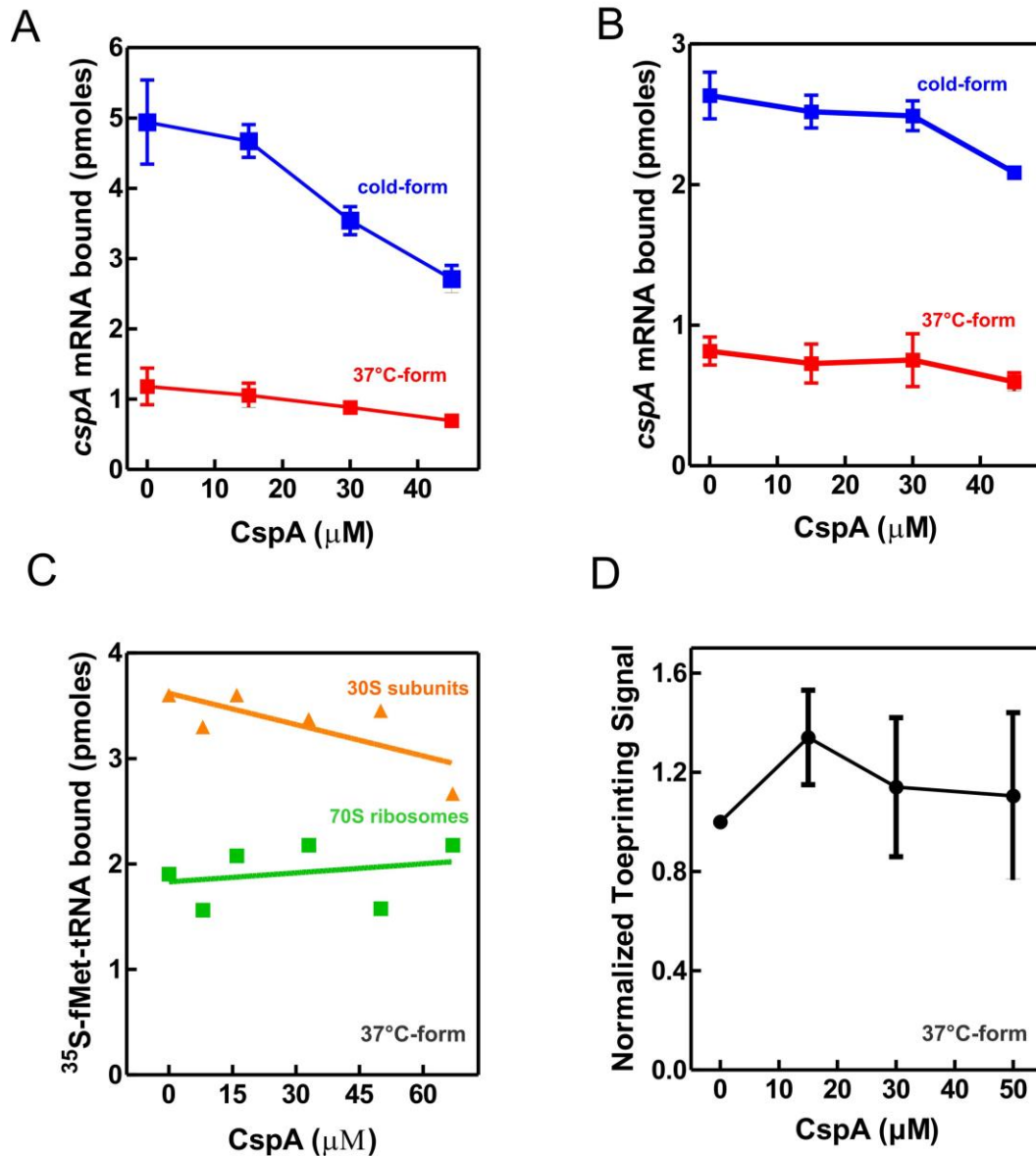


**FIGURE 2. Effect of CspA on the individual steps of translation initiation.** The effect of increasing amounts of CspA on the binding of *cspA* mRNA on the 30S subunits was monitored at 15°C by filter binding of <sup>32</sup>P-labelled *cspA* mRNAs folded in the cold-form (blue) or in the 37°C-form (red) in the absence (A) or in the presence (B) of IFs and fMet-tRNA<sup>Met</sup>. The effect of increasing amount of CspA on the initiation phase of translation at 15°C was also investigated by analyzing: (C) the binding of <sup>35</sup>S-fMet-tRNA<sup>Met</sup> to 30S subunits (green squares) and to 70S ribosomes (orange triangles) programmed with IFs and the 37°C-form of *cspA* mRNA by filter binding assay and (D) the localization of 30S on the translation start site of *cspA* mRNA by toeprint assay. The data points in panels A, and B are the average of triplicates. The data points in panel D result from the quantification of toeprint signals of two independent experiments. Error bars represent the standard deviations. Further details are given in Materials and Methods.

301 ribosomal A site in the absence of the cognate A-site tRNA (Pedersen et al., 2003;  
302 Neubauer et al., 2009), in a so-called “RelE walking” experiment. Radiolabeled cold- and  
303 37°C-forms of *cspA* mRNA were translated *in vitro* at 15°C using the PURE system (NEB)  
304 – a reconstituted system of the *E. coli* translation machinery with reduced concentration of  
305 charged asparagine tRNA (Asn-tRNA<sup>Asn</sup>) (Shimizu et al., 2001 and patent US7118883b2).  
306 At the end of the incubation, chloramphenicol and RelE were added to the reaction  
307 mixtures to stabilize the polysomes and to cut the mRNA at the codons in which the  
308 ribosomes were blocked due to the low content of Asn-tRNA<sup>Asn</sup>, respectively. Using  
309 polyacrylamide gel electrophoresis (PAGE), we monitored the extent of RelE cleavages on  
310 the three Asn triplets AAC (13<sup>th</sup>, 39<sup>th</sup> and 66<sup>th</sup> codon) and on the first A-site codon after the  
311 AUG. This experiment provides new data concerning the fraction of ribosomes engaged in  
312 mRNA translation and the ribosomal progression along the transcript.

313 Figure 3A shows that RelE cleaves extensively all Asn codons of the cold *cspA*  
314 mRNA form, independently of CspA, confirming its translability at low temperature.  
315 Interestingly, the intensities of the RelE cleavages detected with the 37°C-form of *cspA*  
316 mRNA (Fig. 3B) are much weaker compared to those of the cold form, the only exception  
317 being the cuts at the first A-site codon, which are comparable in the two forms of *cspA*  
318 mRNA. The data suggest that the number of ribosomes transiting along *cspA* mRNA and  
319 pausing at the asparagine codons is significantly lower in the case of the highly structured  
320 37°C-form than in the cold-form of the mRNA. Notably, the addition of CspA to the  
321 translation system programmed with the 37°C-form causes intensification of the RelE  
322 cleavages, suggesting that the number of elongating ribosomes has enhanced (Fig. 3B).  
323 Indeed, quantification of the gel bands (Fig. 3C and 3D, normalized values) reveals that  
324 CspA induces on average a 2.5-fold increase of progression with the 37°C-form, a value  
325 very close to the observed stimulatory effect on translation (Fig. 1D). The fact that CspA  
326 does not affect the rate of RelE cleavage of the cold-form of *cspA* mRNA (Fig. 3C)

327

328

329

330

331

332

333

334

335

336

337

338

339

340

341

342

343

344

345

346

347

348

349

350

351

352

353

354

355

356

357

358

359

360

361

362

363

364

365

366

367

368

369

370

371

372

373

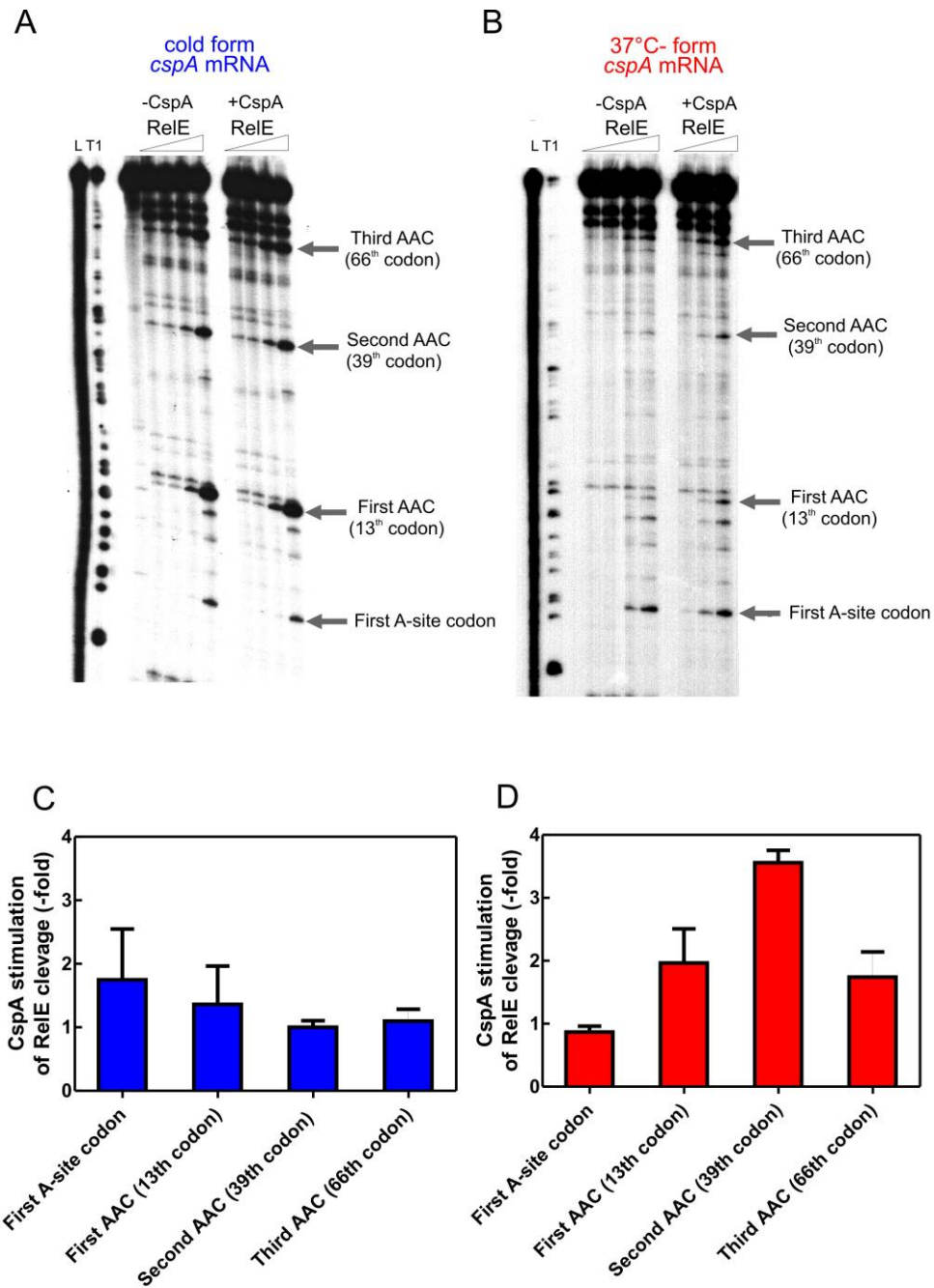


**FIGURE 3. RelE walking experiment.** <sup>32</sup>P-labelled *cspA* mRNA, folded in the cold-structure (A) or in the 37°C-structure (B), was used as templates for an *in vitro* translation assay with the PURE system and then cleaved with 0, 0.16, 0.72 and 1.44 μM of RelE. Lane L: alkaline ladder; lane T1: RNase T1 ladder. The first A-site codon (after the AUG initiation codon) and the AAC codons specifying Asn are indicated. Numbering is given according to the initiation codon. C and D show the effect of CspA (30 μM) on the intensity of RelE cleavages (normalized to the total radioactivity present in each lane) on the 15°C- and 37°C-structures, respectively. Averages of the fold changes observed using the three different RelE concentrations are reported with standard deviations.

374 excludes the possibility that CspA could influence directly the RelE activity on the 37°C-  
375 form. The fact that the 3' termini of the two *cspA* mRNAs are identical (Giuliodori et al.,  
376 2010) excludes the possibility that the diverse RelE cleavage rates between the two forms  
377 could be promoted by a different rate of ribosome recycling. Finally, the RelE cuts at the A-  
378 site of the 70S initiation complex are similar in the absence and in the presence of CspA,  
379 thus ruling out the possibility that CspA could favor the occupancy of the A site by the aa-  
380 tRNA in the initiation phase.

381 Based on the RelE walking experiments, we propose that CspA promotes  
382 progression of the ribosomes on structured mRNAs during translation elongation at low  
383 temperature.

384

#### 385 *Binding of CspA to cspA mRNA is responsible for translation stimulation*

386

387 Isothermal Titration Calorimetry (ITC) is a powerful technique for studying  
388 interactions between native proteins and their RNA targets (Klebe et al., 2015). We used  
389 this approach to probe the possible interaction of CspA with the 70S ribosome (Fig. 4A),  
390 individual 30S (Fig. 4B), and 50S subunits (Fig. 4C) at 15°C, 25°C, and 35°C (Fig. 4-figure  
391 supplement 1). We fail to detect a specific interaction between CspA with either the 70S  
392 ribosome or the isolated subunits. The small variations observed are due to the heat  
393 released by the disassembly of CspA or ribosome aggregates in buffer upon dilution (Fig.  
394 4-figure supplement 1). On the other hand, as expected, we detected the specific binding  
395 of initiation factor IF1 to the 30S subunit at low temperature under comparable conditions  
396 ( $K_d = 806$  nM). Notably, IF1 and CspA share impressive structural similarity (Gualerzi et  
397 al., 2011) and are both RNA binding proteins (Phadtare and Severinov, 2009); however,  
398 IF1 overexpression in *E. coli* does not suppress the defects of the *csp* quadruple deletion  
399 strain (Phadtare and Severinov, 2009).

400

401  
402  
403  
404  
405  
406  
407  
408  
409  
410  
411  
412  
413  
414  
415  
416  
417  
418  
419  
420  
421  
422  
423  
424  
425  
426  
427  
428  
429  
430  
431  
432  
433  
434  
435  
436  
437  
438  
439  
440  
441  
442  
443  
444  
445  
446  
447

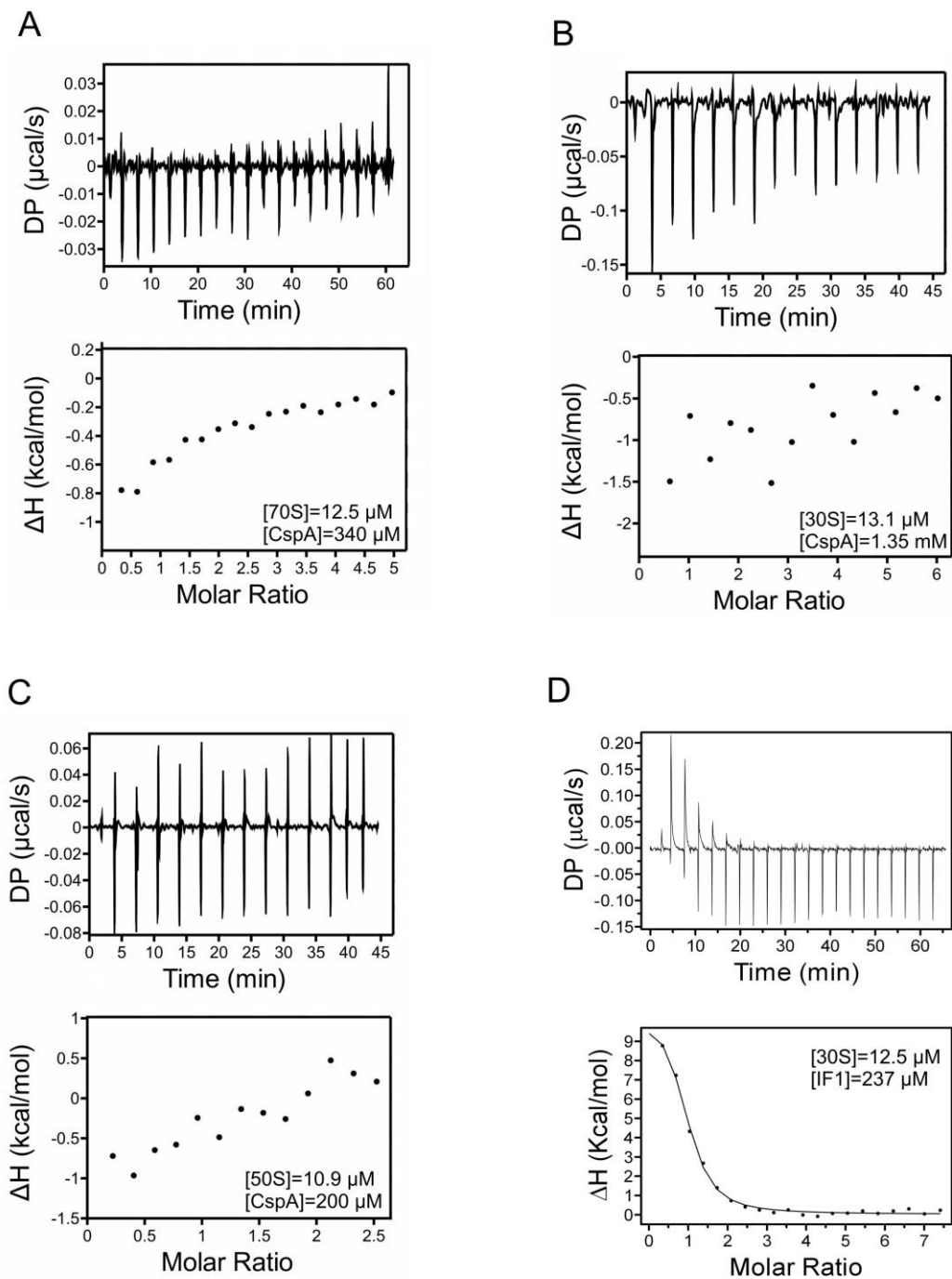
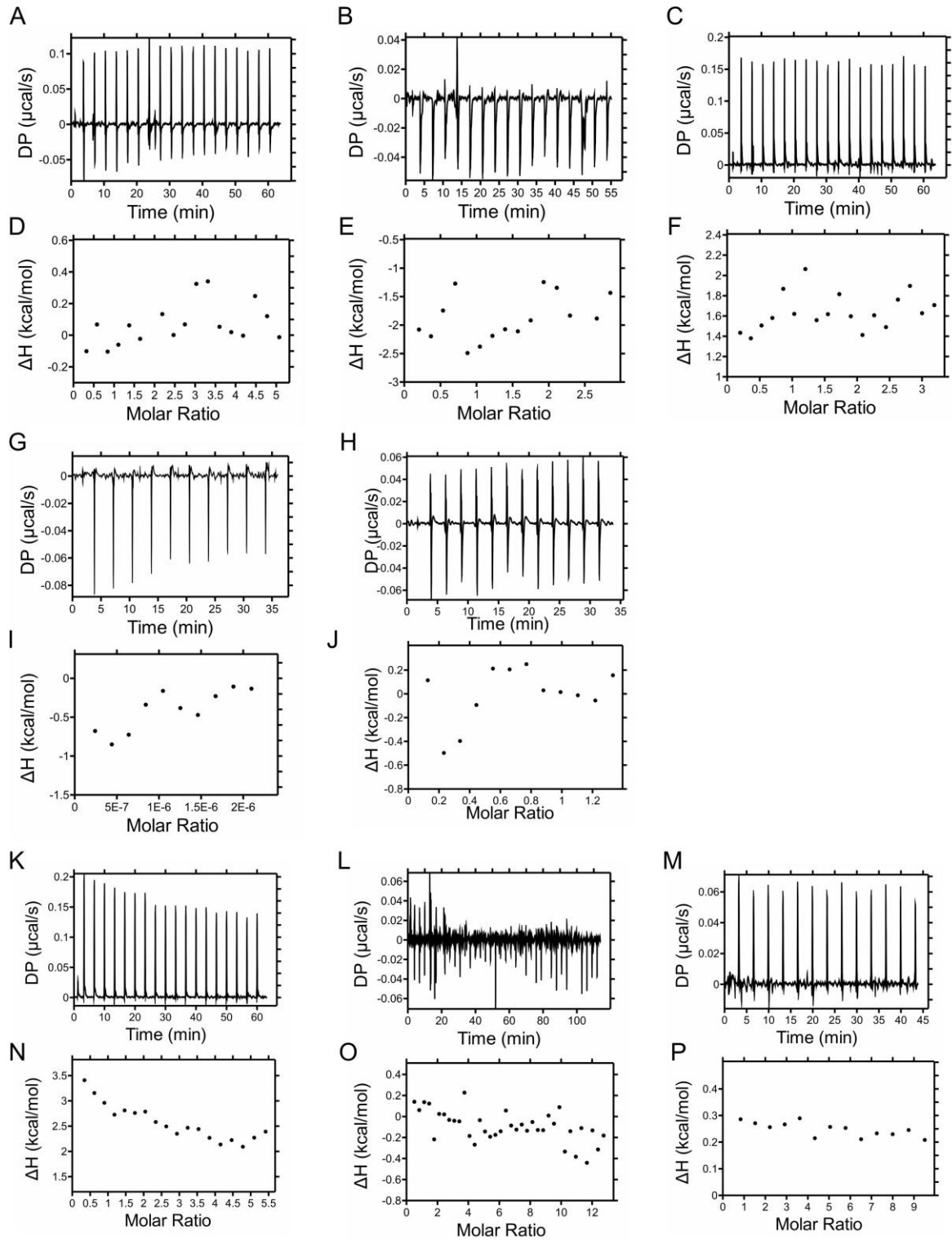


**FIGURE 4. ITC analysis of CspA interaction with the 70S ribosomes and ribosomal subunits.** Titration of *E. coli* ribosomes with CspA was studied at 15°C by sequential 2  $\mu\text{L}$  injections of CspA in a cell containing 200  $\mu\text{L}$  of 70S ribosomes (A), 30S subunits (B) or 50S subunits (C). Control experiments were performed using IF1 and 30S subunits at the indicated concentrations (D).



448  
449  
450  
451  
452  
453  
454  
455  
456  
457  
458  
459  
460  
461  
462  
463  
464  
465  
466  
467  
468  
469  
470  
471  
472  
473  
474  
475  
476  
477  
478  
479  
480  
481  
482  
483



484 **FIGURE 4-supplement 1. Binding of CspA to 70S ribosomes or ribosomal subunits.** Titration  
485 of *E. coli* ribosomal particles with CspA was studied at 25°C (A-E) and 35 °C (F-H). Titration  
486 was carried out by consecutive 2  $\mu\text{L}$  injections of CspA in a cell containing 200  $\mu\text{L}$  of either 70S  
487 ribosomes (A, and F), 30S subunits (B and G) or 50S subunits (C and H). D and E are examples of  
488 signals of CspA and *E. coli* 50S subunits obtained upon dilution in ITC buffer at 25 °C: in (D) 2  $\mu\text{L}$   
489 of CspA were repeatedly injected in the sample cell filled with ITC buffer, while in (E) 2  $\mu\text{L}$  of ITC  
490 buffer were repetitively injected in the sample cell filled with 50S subunits.

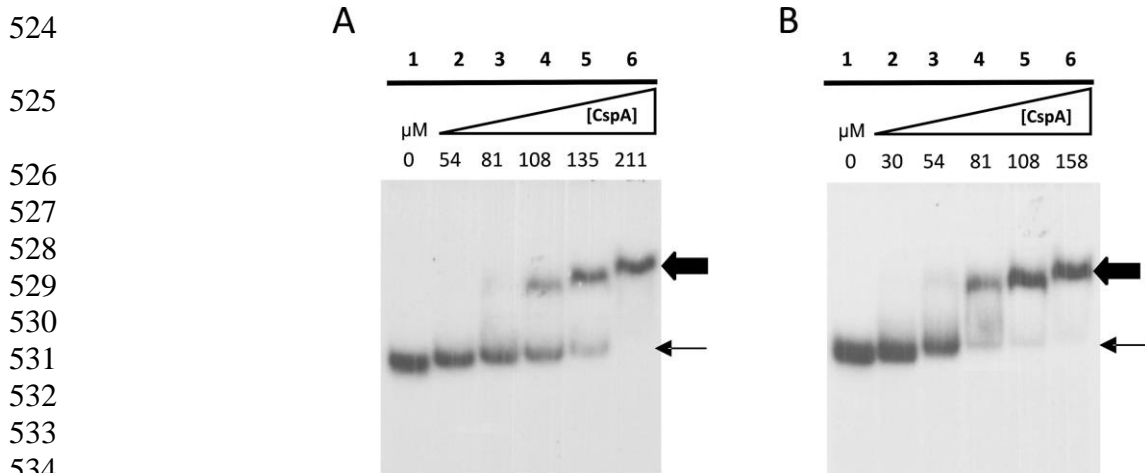
491  
492



493 CspA has been shown to bind RNA including the 5'-UTR of its own transcript (Jiang  
494 et al. 1997). Therefore, we investigated CspA-*cspA* mRNA interaction using  
495 Electrophoresis Mobility Shift Essay (EMSA). Given the large size (428 nts) of the full-  
496 length *cspA* transcript and the small mass of CspA (7.4 KDa), separation of such  
497 complexes constituted a technical challenge. Therefore, the analysis was done using a  
498 *cspA* mRNA fragment of 187 nts (*187cspA* RNA) consisting of the whole 5' UTR plus 27  
499 nts of the coding region. Importantly, this fragment adopts a secondary structure highly  
500 similar to that found in the full-length transcript at low temperature (Giuliodori et al., 2010).  
501 Complex formation with increasing concentrations of CspA is shown in in Fig. 5A and B.  
502 Below 80  $\mu$ M of CspA, a complex with minor gel retardation is observed (indicated with a  
503 thin arrow). However, as the amount of CspA exceeds 80  $\mu$ M, a super-shifted band  
504 appears (indicated with a thick arrow), whose mobility continues to decrease with  
505 increasing amounts of CspA. This result indicates that the *187cspA* RNA contains multiple  
506 binding sites for CspA that are progressively occupied as the concentration of the protein  
507 rises. The appearance of the super-shift supports the hypothesis of a cooperative binding  
508 to RNA by CspA (Jiang et al., 1997; Lopez and Makhatadze, 2000). These experiments  
509 demonstrate that multiple CspA bind to its mRNA at both low (Fig. 5A) and high  
510 temperatures (Fig. 5B) and confirm that this protein can bind also structured RNA  
511 molecules, although in this case the multi-protein complexes are formed only at high  
512 protein concentrations.

513 The details of the CspA:*cspA* mRNA interaction at 15°C were then dissected using  
514 three different approaches: (i) UV-induced cross-linking and (ii) enzymatic probing, and  
515 Fe-EDTA footprinting. The resulting cross-link and footprint patterns are reported in the  
516 structure models of the cold-form (Fig. 6) and the 37°C-form (Fig. 7) of *cspA* mRNA, while  
517 the electrophoretic analyses are shown in Fig. 7-figures supplement 1, 2 and 3. In the  
518 cold-form, we identified 11 main sites, which were either protected or cross-linked to CspA.

519 Overall, the CspA sites are mainly positioned in apical or internal loops, extending also into  
520 the adjacent helices. Most of these sites are rather large, especially sites 1, 7, 9 and 10,  
521 which are located at positions 12-36, 170-186, 266-281 and 321 to 337, respectively.  
522 Notably, the CspA-induced cross-links at sites 7, 9 and 10, which also overlap with CspA  
523 induced protections against enzymatic cleavages or FE-EDTA, are particularly strong.



539 **FIGURE 5. CspA-187cspA RNA interaction studied by EMSA.** The binding of CspA to <sup>32</sup>P-  
540 labeled 187cspA RNA performed at 20°C (A) or at 37°C (B) was analyzed in gel retardation assays  
541 as described in Materials and Methods using the concentrations of protein indicated at the top of  
542 the gels. The thin and thick arrows indicate the complexes with high and low mobility, respectively.  
543

544 Probing the 37°C-form of *cspA* mRNA bound to CspA shows significantly different  
545 patterns as compared to the cold-form. Only 5 of the 11 sites present in the cold-form had  
546 a counterpart in the 37°C-form, namely sites 1, 3, 4, 7 and 10, while the other regions  
547 became insensitive to CspA (sites 2, 5, 6, 8, 9, and 11). Furthermore, the binding sites  
548 were shorter as compared to the cold-form, with the exception of site 7 at the beginning of  
549 the coding region, which remained quite extended. Finally, the cross-links were overall  
550 less intense and much more dependent upon CspA concentration than in the case of the  
551 cold-form.

552 The above-described differences can be likely attributed to the more compact  
553 structure of the 37°C-form, characterized by a long helix interrupted by several internal  
554 loops and bulged bases formed by the interaction between the 5' UTR and part of the  
555 coding region (nucleotides C232 to G326). This closed conformation is further stabilized at  
556 low temperature (15°C) at which the probing experiments were performed. Indeed, the  
557 reduced binding of CspA to the 37°C-form mRNA is not surprising considering the  
558 preference of Csp proteins for single stranded nucleic acids. Most likely, CspA needs  
559 unstructured regions for the initial contacts with the target RNA.

560

#### 561 *Binding of CspA to a short cspA mRNA fragment affects the mRNA conformation*

562 The secondary structure of three *cspA* mRNA fragments of increasing length (i.e. 87,  
563 137 and 187 nts) from the transcriptional start site was previously analysed (Giuliodori et  
564 al., 2010). These *cspA* mRNA fragments were designed as representative of RNA folding  
565 intermediates occurring during transcription. Their structures do not vary with temperature,  
566 and the 137*cspA* and 187*cspA* fragments adopt similar folding as in the full length cold-  
567 form of *cspA* mRNA. To investigate the role played by CspA on the initial mRNA folding  
568 process, we have analyzed the footprint of CspA on both the 87*cspA* and the 137*cspA*  
569 RNA fragments using RNase V1 (specific of double-stranded regions), RNase T1 (specific

570

571

572

573

574

575

576

577

578

579

580

581

582

583

584

585

586

587

588

589

590

591

592

593

594

595

596

597

598

599

600

601

602

603

604

605

606

607

608

609

610

611

612

613

614

615

616

617

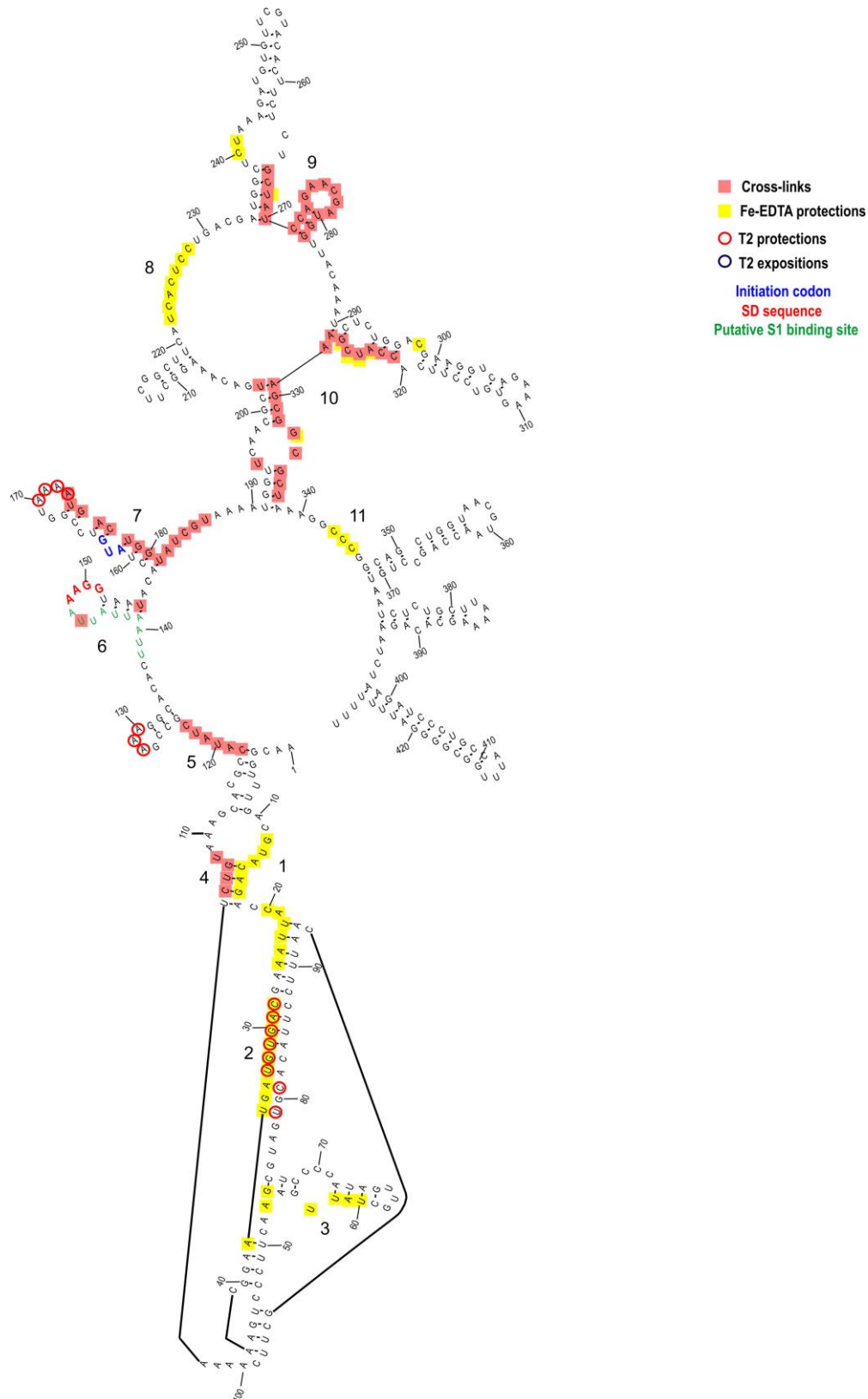


**FIGURE 6. CspA-binding sites identified on the cold-form of *cspA* mRNA.** The footprinted/crosslinked positions reported on the structural model derive from the probing experiments performed at 15°C using the *cspA* mRNA folded in the cold-conformation. The SD sequence (red), the start codon (blue) and the putative S1-binding site (green) are indicated. The secondary structure model of *cspA* mRNA is taken from Giuliodori et al., 2010.

618

619

620

621

622

623

624

625

626

627

628

629

630

631

632

633

634

635

636

637

638

639

640

641

642

643

644

645

646

647

648

649

650

651

652

653

654

655

656

657

658

659

660

661

662

663

664

665

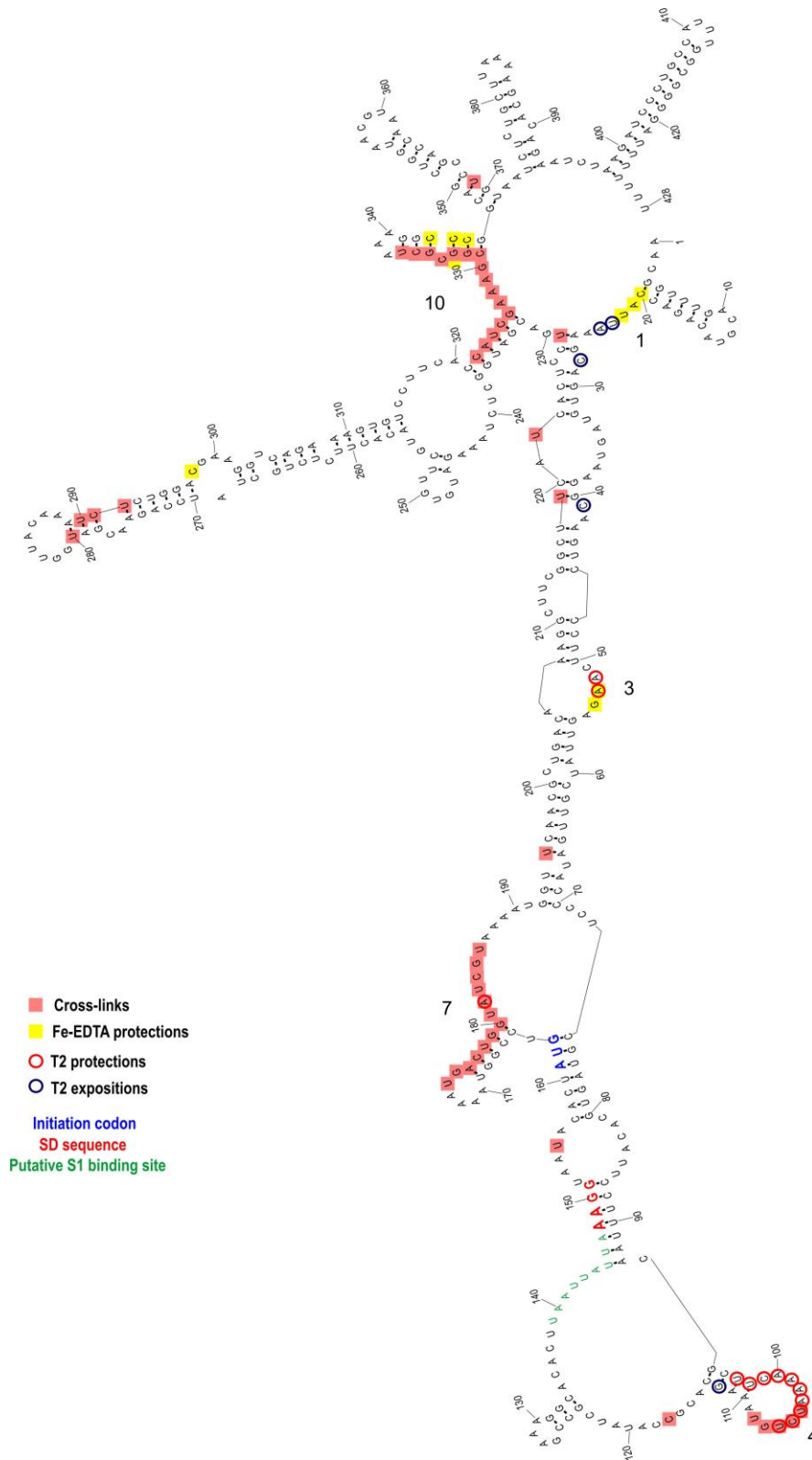


**FIGURE 7. CspA binding sites identified on the 37°C-form of *cspA* mRNA.** The footprinted/crosslinked positions reported on the structural model derive from the probing experiments performed at 15°C using the *cspA* mRNA folded in the 37°C-conformation. The SD sequence (red), the start codon (blue) and the putative S1-binding site (green) are indicated. The secondary structure model of *cspA* mRNA is taken from Giuliodori et al., 2010.

666  
667  
668  
669  
670  
671  
672  
673  
674  
675  
676  
677  
678  
679  
680  
681  
682  
683  
684  
685  
686  
687  
688  
689  
690  
691  
692  
693  
694  
695  
696  
697  
698  
699  
700  
701  
702  
703  
704  
705  
706  
707  
708  
709  
710  
711  
712  
713  
714  
715

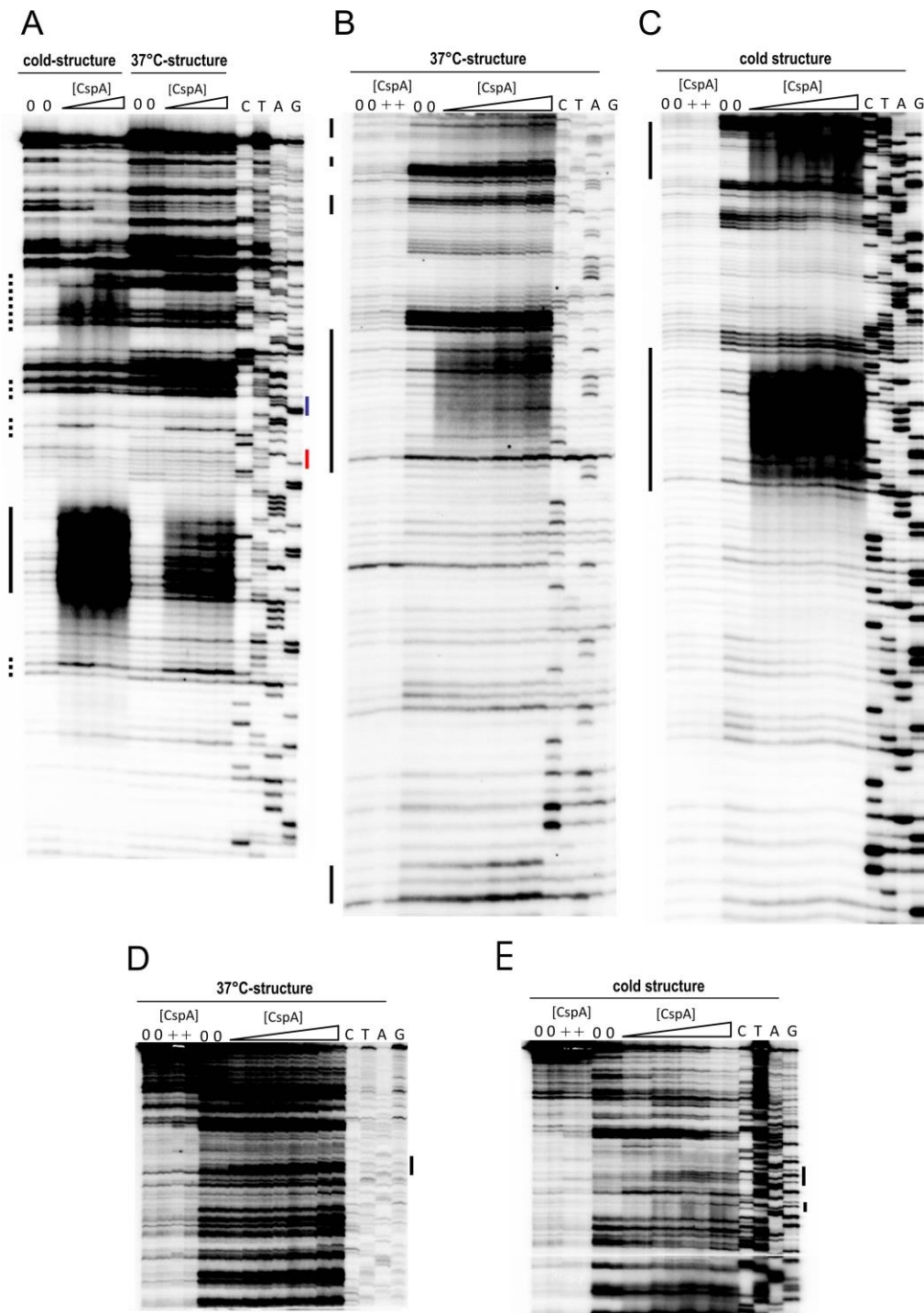


**FIGURE 7-supplement 1. Localization of CspA binding sites on *cspA* mRNA by UV-induced cross-linking at 15°C.** The experiments were performed in the absence (lanes 0) or in the presence of 28 and 57  $\mu\text{M}$  of CspA (panel A) or 28, 57, 115, 170  $\mu\text{M}$  of CspA (panels B, C, D, and E) with *cspA* mRNA folded in the conformations indicated at the top of the gels. Lanes C: mRNA alone, no cross-links; lanes +: mRNA+170  $\mu\text{M}$  of CspA, no cross-links. Increasing concentrations are indicated with a triangle. All conditions are in duplicate. Lanes C, T, A, and G correspond to sequencing reactions. Primer extension analysis was performed using primer *csp2* (panel A), which annealed to the coding region and primer *csp3* (panels B, C), which annealed to the 3' UTR. Panels D and E show the upper parts of the gels displayed in panels B and C. Bases whose accessibility to the cleavage is affected by CspA are highlighted by black bars on the left side of the gels. The blue and red bars on the right side of panel A indicate the Shine-Dalgarno sequence and the AUG initiation triplet, respectively.



716  
717

718  
719  
720  
721  
722  
723  
724  
725  
726  
727  
728  
729  
730

731

732

733

734

735

736

737

738

739

740

741

742

743

744

745

746

747

748

749

750

751

752

753

754

755

756

757

758

759

760

761

762

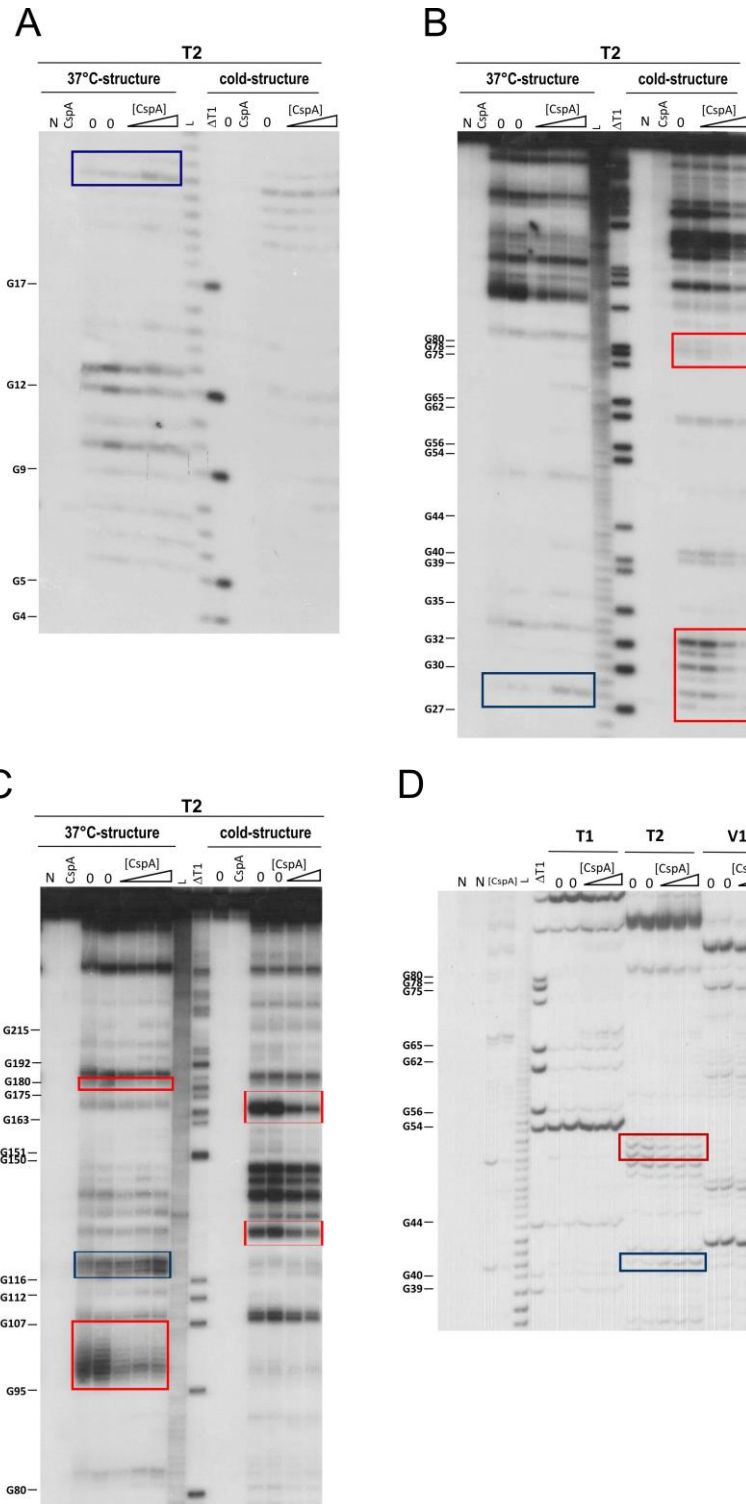


**FIGURE7-supplement 2. Footprinting experiments using RNases.** Short (A and B) and long (C) electrophoretic migration of the fragments generated by RNase T2 (T2) digestion of 5'-end [<sup>32</sup>P]-labelled *cspA* mRNA folded in the conformations indicated at the top of the autoradiographies; (A) bottom and (B) top of the gel. (D) Short electrophoretic migration of the fragments generated by RNases T1, T2, and V1 digestion of 5'-end [<sup>32</sup>P]-labelled *cspA* mRNA folded in the 37°C-conformation. The experiment was carried out at 15°C in the absence (lanes 0) or in the presence of 80, 102, 160 μM of CspA (increasing concentrations are indicated with a triangle). Lanes N: controls with neither T2 nor CspA; lanes +: controls without T2, with CspA; lanes T: RNase T1 cleavages under denaturing conditions; lanes L: alkaline ladder. The red and blue boxes indicate the positions protected or exposed by CspA, respectively.



763  
764

765  
766  
767  
768  
769  
770  
771  
772  
773  
774  
775  
776  
777  
778  
779  
780  
781  
782  
783  
784  
785  
786  
787  
788  
789  
790  
791  
792  
793  
794  
795  
796  
797  
798  
799  
800  
801  
802  
803  
804  
805  
806  
807  
808  
809  
810  
811  
812  
813

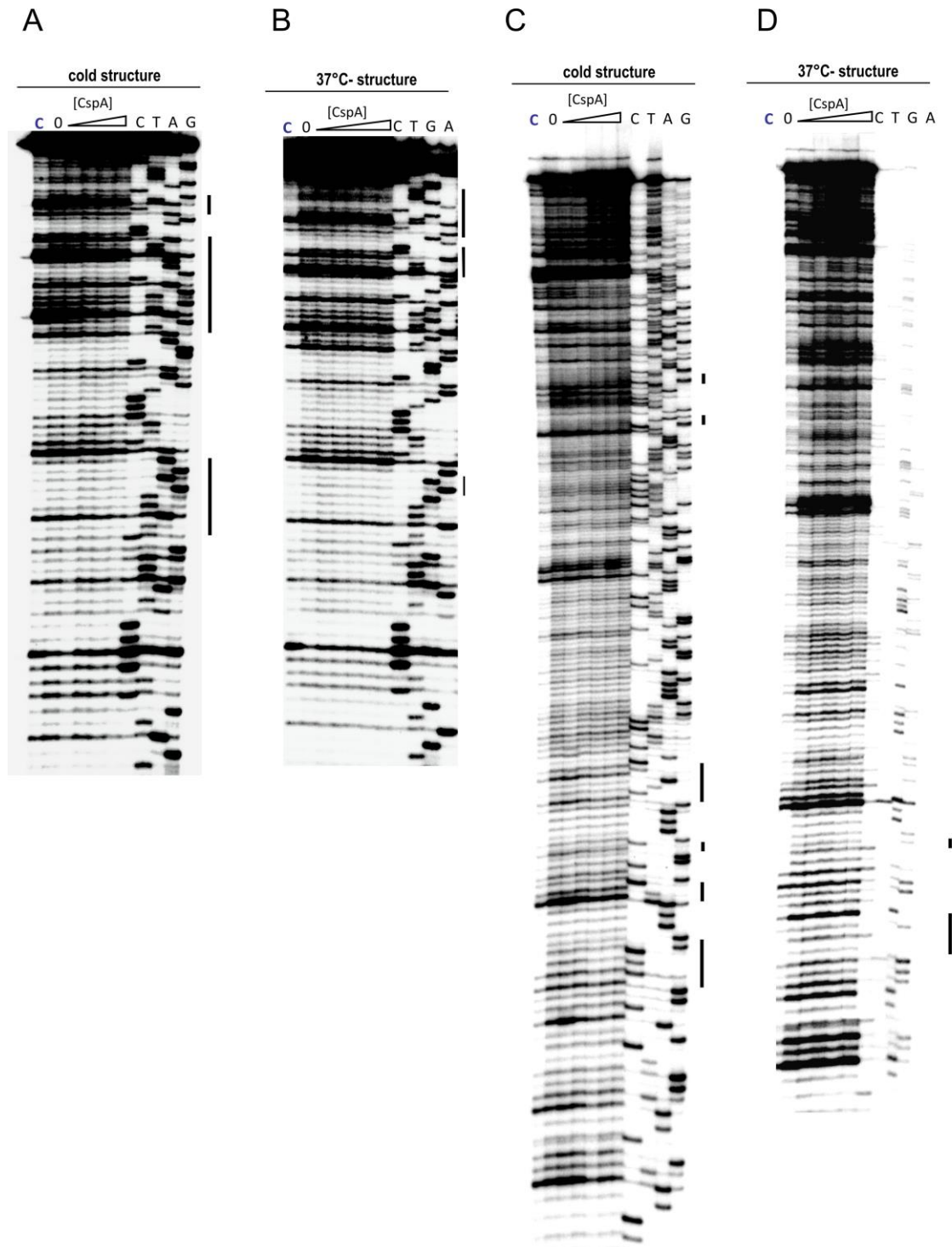


**FIGURE 7-supplement 3. Effect of CspA on the *in situ* accessibility of *cspA* RNA to hydroxyl radical cleavage.** Primer extension analysis of the cleavage sites generated by hydroxyl radicals on *cspA* mRNA folded in the conformations indicated at the top of the gels, in the presence of increasing concentrations of CspA (0, 15, 30, 60, 120  $\mu$ M; increasing concentrations are indicated with a triangle). Lanes C: uncleaved mRNA. Lanes C, T, A, and G correspond to sequencing reactions. Primer extension analysis was performed using primer *csp1* (panels A and B), which annealed to the 5' UTR, and primer *csp3* (panels C and D), which annealed to the 3' UTR. Bases whose accessibility to the cleavage is affected by CspA are highlighted by black bars on the right side of the gels.

814 of unpaired guanine), and RNase T2 (specific of unpaired A>U>C). Binding of CspA to the  
815 short *87cspA* RNA significantly affects the RNase cleavage pattern, but only at a  
816 concentration of CspA above 50  $\mu$ M (Fig. 8A). For instance, protections against RNase T2  
817 were observed between A29 and U33, and at positions U58 and U76; concomitantly  
818 enhanced RNase cleavages were found at positions C41, C50, A51, G65 and C81-A82.  
819 On the other hand, the addition of high concentrations of CspA had only minor effects on  
820 the structure of *137cspA* RNA (Fig. 8B and supplemental 1). For instance, the CspA-  
821 dependent protections in the region A29 and U33 of *87cspA* RNA were no longer  
822 observed.

823 These data suggest that CspA might have different functional impacts *in vivo* during  
824 the transcription process of *cspA* that will depend on many factors including CspA  
825 concentration, and kinetics of RNA transcription and folding.

826

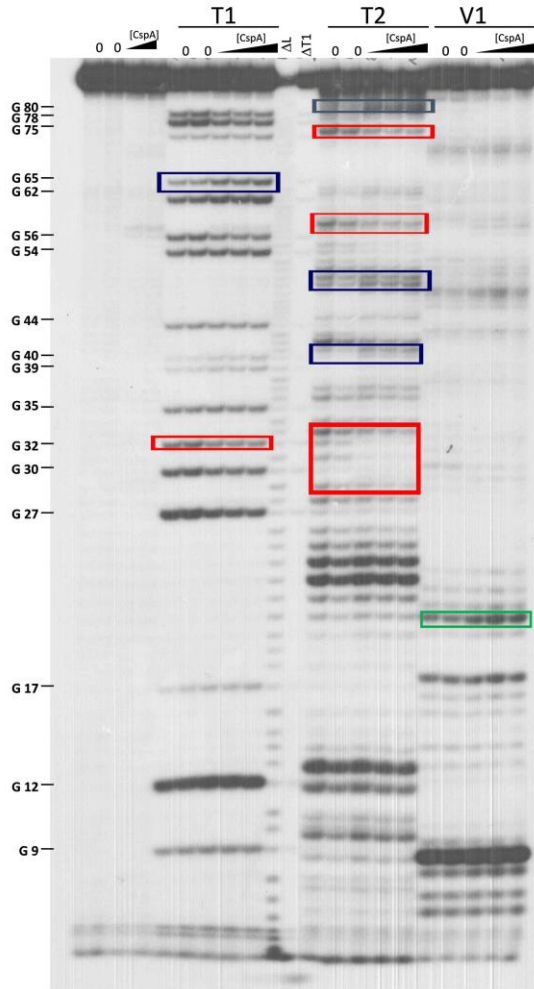
### 827 *CspA preferentially binds to short RNA sequences containing YYR motif*

828 Inspection of all sites covered by CspA revealed that 11 out of 15 of these regions  
829 comprise an YYR (pyrimidine-pyrimidine-purine) motif. Multiple alignments were performed  
830 using the YYR motif as the reference sequence (Fig. 9A). Although the motif is highly  
831 degenerated, the YYR motif seems not to be followed by a G two positions downstream  
832 from the R. The degree of specificity of CspA for the identified sequence features was then  
833 tested by tryptophan fluorescence titration experiments using an RNA oligonucleotide  
834 (Oligo1: 5'-AAC**UG**GUA-3') whose sequence reflected the conserved positions as shown  
835 in Figure 9B. The experiment was also performed with 5 other RNA oligos in which each  
836 one of the bases located in the central positions of Oligo1 was individually replaced by A.  
837 In addition, a poly-A oligo was also used. The data (Fig. 9C and Table 1) show that the  
838 single nucleotide changes caused only small variations of the dissociation constant ( $K_D$

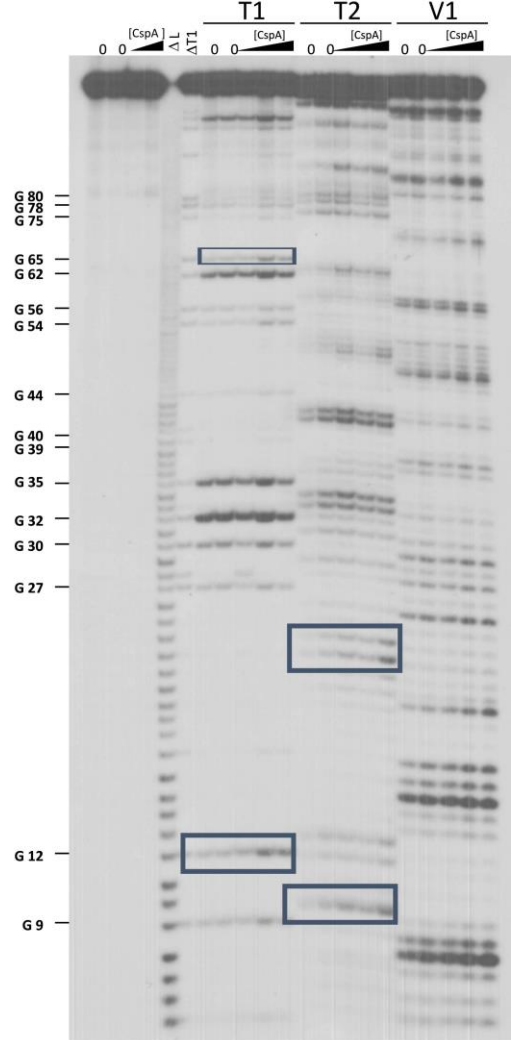
839 around 1  $\mu$ M), with the exception of oligo 6 (G replaced by A at position 6), which  
 840 produced a 5-fold increase

841

A



B



843

844

845

846

847

848

849

850

851

852

853

854

855

856

857

858

859

860

861

862

863

864

865

866

867

868

869

870

871

872

873

874

875

876

877

878

879

880

881

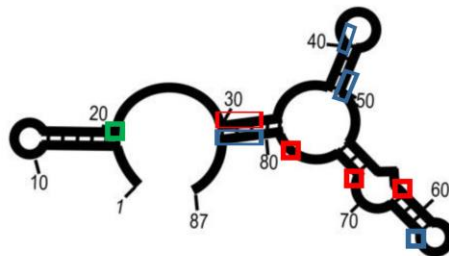
882

883

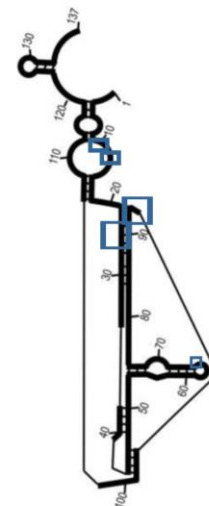
884

885

C



D



886 **FIGURE 8. Footprinting experiments of fragments 87cspA and 137cspA RNAs.** (A) Short  
887 electrophoretic migration of the fragments generated by RNase T1 (T1), RNase T2 (T2) or RNase  
888 V1 (V1) digestion of 5'-end [<sup>32</sup>P]-labelled (A) 87cspA RNA and (B) 137cspA RNA. The experiments  
889 were carried out in the absence (lanes 0) or in the presence of 51, 81, and 105 μM of CspA  
890 (increasing concentrations are indicated with a triangle). Lane ΔT: RNase T1 cleavages under  
891 denaturing conditions; lane ΔL: alkaline ladder. The red and blue boxes indicate the positions  
892 protected or exposed by CspA, respectively, while the green boxes indicate the V1 cuts enhanced  
893 by CspA. The same positions are reported on the schematic structural model (Giuliodori et al.,  
894 2010) of the 87cspA RNA (C) or of the 137cspA RNA (D).  
895  
896  
897

898

899

900

901

902

903

904

905

906

907

908

909

910

911

912

913

914

915

916

917

918

919

920

921

922

923

924

925

926

927

928

929

930

931

932

933

934

935

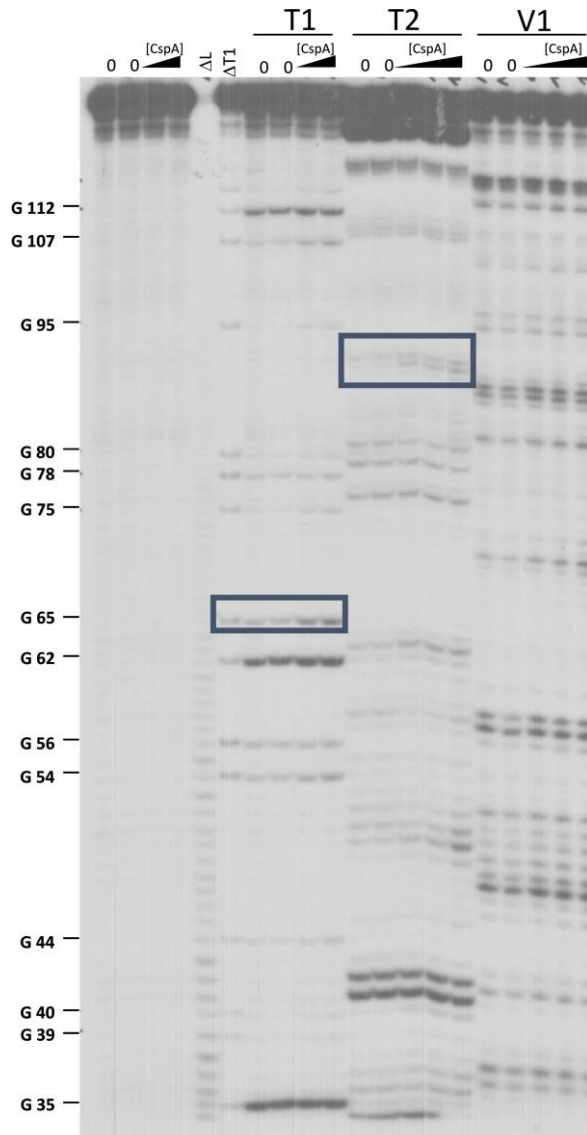


**FIGURE 8 supplement 1.** Long electrophoretic migration of the fragments generated by RNase T1 (T1), RNase T2 (T2) or RNase V1 (V1) digestion of 5'-end [<sup>32</sup>P]-labelled 137cspA RNA. The experiment was carried out as indicated in Fig. 8.

936 of the  $K_D$ . A similar decrease of affinity was observed with the poly-A oligonucleotide.

937 Because there is a high degree of sequence and structure similarity between *E. coli*  
938 CspA and its *B. subtilis* orthologue CspB, we produced a homology model of CspA in  
939 complex with Oligo 1 using the available 3D structure of a CspB-RNA complex (Sachs et  
940 al., 2012). This model (Fig. 9D) allowed us to verify that the YYR core motif, unlike other  
941 combinations of trinucleotides like RRR, fits very well in the binding pocket. From the  
942 model, the sidechains of His33, Phe31, Phe20, and Trp11, would stack with A2, C3, U4,  
943 G5, respectively, while G6 is stacked on G5. Hence, RNA binding is dominated by  
944 stacking interactions between the YYR motif and the aromatic protein sidechains of  
945 Phe31, Phe20 and Trp11. Furthermore, the purine downstream from the YYR motif can  
946 strengthen the stacking of the side chain of Trp11 with G5, while the nucleotide (A/U)  
947 upstream the core motif can stack with the sidechain of His31, further stabilizing the  
948 protein-RNA interaction.

949 Taken together, our data support that the YYR might be the preferred seed sequence  
950 to initiate binding. They are also in agreement with earlier works (Jiang et al., 1997; Lopez  
951 and Makhatadze, 2000) reporting the  $K_D$  for the CspA-RNA complex in the  $\mu\text{M}$  range.

952

953 **Table 1. Equilibrium dissociation constants of the CspA:RNA oligonucleotide**  
954 **complexes determined by tryptophane fluorescence titration.**

955

956

957

958

959

960

961

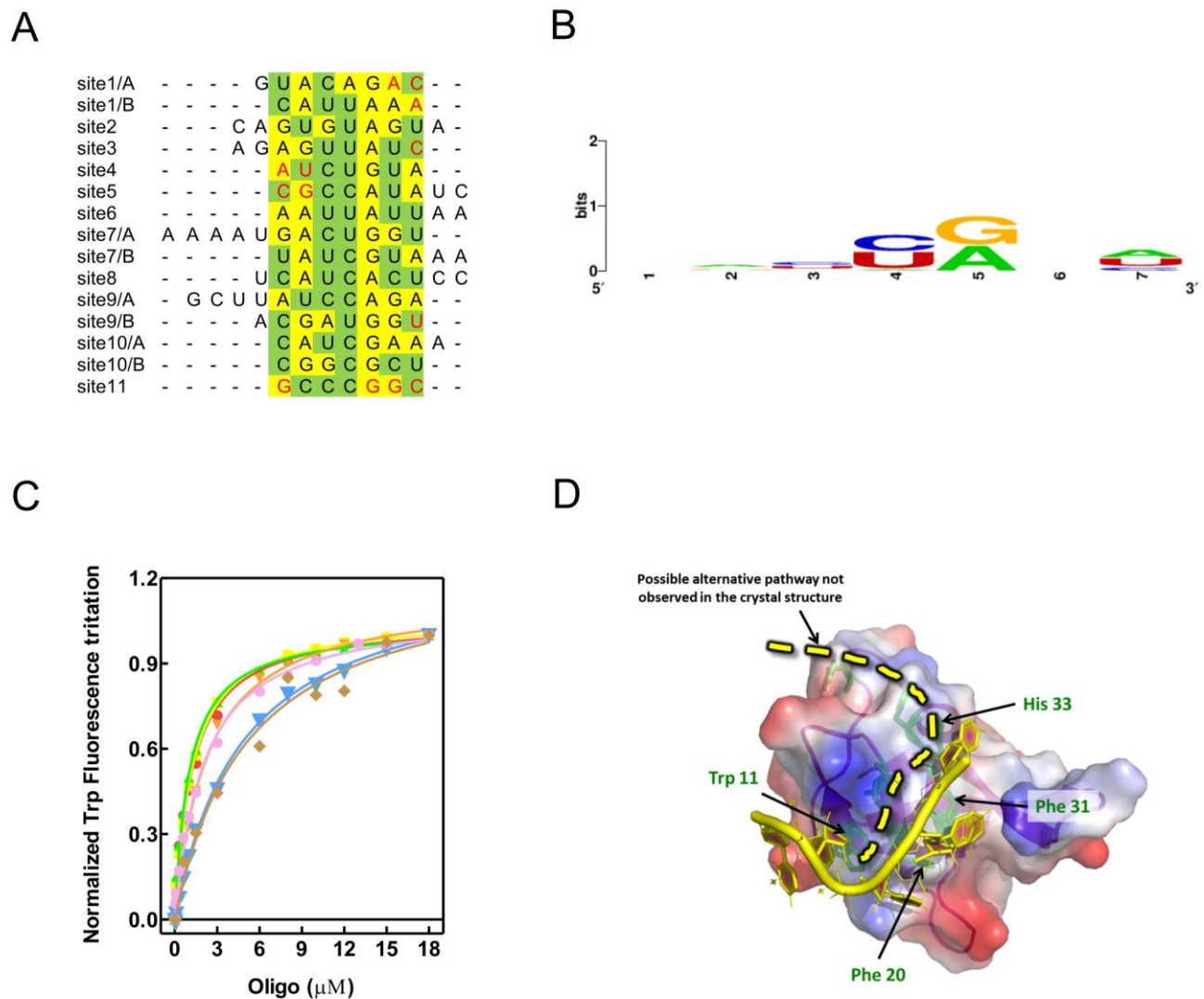
962

963

964

Oligonucleotide	Sequence 5' to 3'	$K_D$ , $\mu\text{M}$
Oligo 1	AACUGGUA	1.24±0.08
Oligo 2	AAAUGGUA	2.30±0.13
Oligo 3	AACAGGUA	1.24±0.05
Oligo 4	AACUAGUA	1.03±0.06
Oligo 5	AACUGAUA	4.86±0.24
Oligo 6	AACUGGAA	2.08±0.14
Oligo 7	AAAAAAAAA	5.13±1.15





965

966 **FIGURE 9. Characterization of CspA-RNA interaction.** (A) Manual multiple alignment of the  
 967 sites cross-linked/footprinted by CspA on *cspA* mRNA. Since CspB, the CspA-homologue of  
 968 *Bacillus subtilis*, recognizes a sequence of 6-7 nts (Lopez and Makhatadze, 2000; Sachs et al.,  
 969 2012), we hypothesized that the sites in which the cross-links/footprints were particularly extended  
 970 (> 12 nts) could be the results of the binding of two adjacent CspA molecules. For this reason, we  
 971 divided these extended sites (sites 1, 7 and 9) into two sub-sequences of comparable length,  
 972 named A and B, which were used to build the alignment. The yellow and green highlighting  
 973 indicates purines and pyrimidine, respectively. The bases in red are adjacent to those  
 974 footprinted/cross-linked by CspA. (B) Logo representation of the CspA binding preference derived  
 975 from the alignment shown in panel A and generated with WebLogo (Crooks et al., 2004). (C)  
 976 Quenching of the CspA Trp fluorescence induced by the binding of oligo1 (5'-AACUGGUA-3', red),  
 977 which contains the most frequent bases found in the conserved positions of the Logo, or by the  
 978 following RNA sequences: oligo2 (5'-AAAUGGUA-3', orange); oligo3 (5'-AACAGGUA-3', yellow);  
 979 oligo4 (5'-AACUAGUA-3', green); oligo5 (5'-AACUGAUA-3', blue); oligo6 (5'-AACUGGAA-3', pink)  
 980 and oligo 7 (5'-AAAAAAAAA-3', brown). Experiments were performed at 20°C in the presence of 1  
 981 μM of CspA and the indicated concentrations of oligos. Further details are given in Experimental  
 982 procedures. (D) Model of CspA-oligoRNA interaction obtained using *B. subtilis* CspB-rC7 structure  
 983 (pdb file 3pf4; Sachs et al., 2012).  
 984

985 *CspA promotes translation of numerous CS and non-CS mRNAs at low temperature*

986 To gain additional insight into the CspA properties we tested the effect of CspA on  
987 the *in vitro* translation of mRNAs other than *cspA*. Two classes of mRNAs were selected to  
988 carry out this analysis: (i) the cold-shock transcripts *cspB* and *P1infA*, the former belonging  
989 to the *E. coli csp* gene family (Yamanaka et al., 1998) and the latter originating from the P1  
990 promoter of *infA* and encoding Initiation Factor 1 (IF1) (Giangrossi et al., 2007); and (ii) the  
991 non-cold-shock transcripts *hupA* and *cspD*, encoding the  $\alpha$ -subunit of the nucleoid  
992 associated protein HU (Giangrossi et al., 2002) and protein CspD (Yamanaka and Inouye,  
993 1997), respectively. As shown in Fig. 10, the translation of *infA* and *cspD* mRNAs is  
994 strongly stimulated by CspA (3-4 fold), that of *cspB* mRNA is moderately enhanced, while  
995 *hupA* mRNA translation is insensitive to CspA addition. This result confirms that CspA is  
996 able to stimulate the translation at low temperature of various transcripts other than its own  
997 mRNA (Giuliodori et al., 2004), but also indicates that this activity cannot be generalized.

998 The existence of the CspA-dependent translational stimulation of the tested mRNAs  
999 (*infA*, *cspD*, *cspB*) raises the question as to whether these transcripts were directly  
1000 recognized by CspA. To address this issue, we mapped the possible interactions between  
1001 CspA and our selected mRNAs by UV-induced crosslinking experiments at 15°C (Fig. 10B  
1002 and Fig. 10-figure supplement 1). Notably, there appears to be a binding site common to  
1003 all tested mRNAs – apart from *cspD* mRNA. The average length of the binding site is of 14  
1004 nts and is located between 9-12 nts downstream from the G of the translation initiation  
1005 codon (Fig. 6, 7, 7 supplement 1, and 10 supplement 1). In the case of *cspD* mRNA,  
1006 multiple cross-links were present along the entire mRNA (Fig. 10-figure supplement 1). In  
1007 the region near the AUG codon, a cross-link of moderate intensity is observed in the SD  
1008 region while a more intense one is located between the 17<sup>th</sup> and the 19<sup>th</sup> codons of the  
1009 coding region. The YYR motif was found also in the regions cross-linked with CspA in  
1010 these mRNAs. The multiple alignments built using the YYR motif as the reference



1011 sequence (Fig. 10C) produced a Logo similar to that generated using the binding sites on  
 1012 *cspA* mRNA (Fig. 10D).

1013  
 1014  
 1015

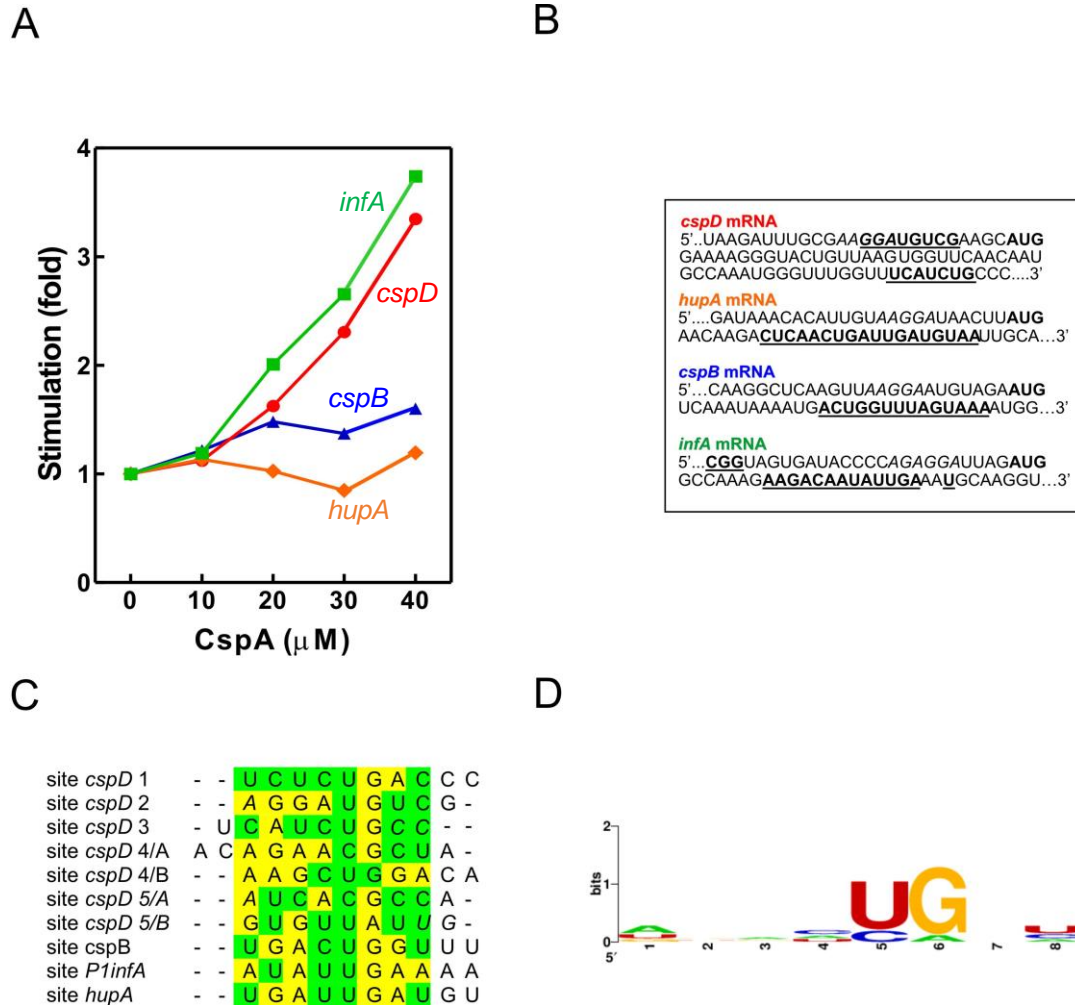


**FIGURE 10. CspA binding to various mRNAs and functional effects.** (A) *In vitro* translation at 15°C performed with control 70S and S100 in the presence of *P1infA* mRNA (green squares), *cspD* mRNA (red circles), *cspB* mRNA (blue triangles), *hupA* mRNA (orange diamonds) and the indicated amounts of purified CspA. (B) CspA binding sites (bold underlined) identified around the Translation Initiation Region (TIR) of the indicated mRNAs by crosslinking experiments performed at 15°C. SD sequence and start codon are indicated in italics and bold, respectively. (C) Multiple alignment of the sites crosslinked by CspA on the indicated mRNAs. As described in the legend of Fig. 9, we divided all sites made up of > 12 nts into two sub-sequences of comparable length, named A and B, which were used to build the alignment. The yellow and green highlighting indicates purines and pyrimidine, respectively. The bases in italics are adjacent to those crosslinked by CspA. (D) Logo representation of the CspA binding preference derived from the alignment shown in panel C and generated with WebLogo (Crooks et al., 2004).

1045

1046

1047

1048

1049

1050

1051

1052

1053

1054

1055

1056

1057

1058

1059

1060

1061

1062

1063

1064

1065

1066

1067

1068

1069

1070

1071

1072

1073

1074

1075

1076

1077

1078

1079

1080

1081

1082

1083

1084

1085

1086

1087

1088

1089

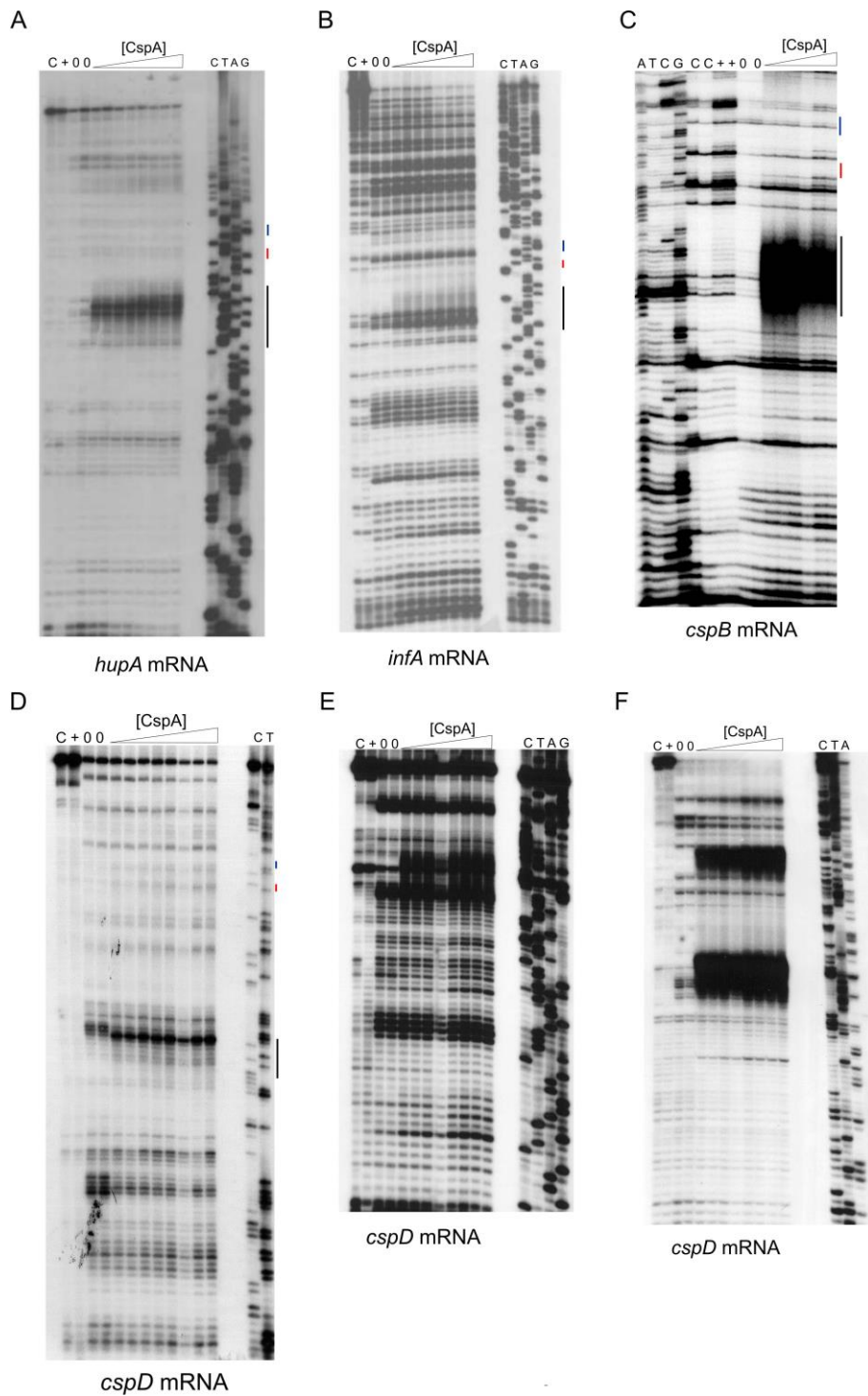


**FIGURE 10 supplement 1. Localization of CspA binding sites on *P1infA*, *cspB* and *hupA* and *cspD* mRNAs by UV-induced crosslinking at 15°C.** The experiment was performed in the presence of 0, 28, 57, and 120  $\mu$ M of CspA. Lanes C: mRNA alone, no cross-links; lanes +: mRNA+120  $\mu$ M of CspA, no cross-links. Increasing concentrations are indicated with a triangle. Lanes C, T, A, and G correspond to sequencing reactions. Primer extension analysis was performed: using primers (A) *hupA* (5'-CTCTGGAGTCCACTCTGGCTG-3'), (B) *P1infA* (5'-GTTCCGCGTAGAGTTAGAAAACG-3'), and (C) *cspB* (5'-GGTAGTAAAGATGTGTTTGTG-3'), which annealed 75, 62, and 70 nts downstream from the initiation codon of the corresponding mRNAs, respectively. Primer extension analysis on *cspD* mRNA was performed using primers: (D) *cspD3* (5'-CAGATGGATGGTTACAGAACGC-3'), which annealed in the middle of the coding region, (E) *cspD4* (5'-GGAAAAGGGTACTGTTAAGTG-3') which annealed immediately downstream from the initiation codon, and (F) primer *cspD2* (5'-GTCTCATTGTGTACATCCTAAAG-3'), which annealed to the 3' UTR.

## 1090 **DISCUSSION**

### 1091 *The CspA paradox*

1092 Our data demonstrate that the binding of CspA to mRNA is not always accompanied  
1093 with an effect on translation. This was particularly well illustrated with *cspA* mRNA: despite  
1094 the extensive binding of CspA to the cold-form of *cspA* mRNA, translation of this structure  
1095 is not stimulated, whereas the translation of the 37°C-form is enhanced by CspA although  
1096 CspA binding is less efficient. How can this apparent paradox be explained?

1097 Immediately after cold-shock CspA becomes a very abundant protein (Brandi et  
1098 al.,1999), and it is estimated to be bound in several copies to cellular mRNAs (Ermolenko  
1099 and Makhatadze, 2002). CspA was shown to bind its own mRNA (Jiang et a., 1997) and to  
1100 act as an RNA chaperone (Jiang et a., 1997; Rennella, 2017; Zhang et al., 2018). In this  
1101 work, we demonstrated that CspA is able to recognize in its mRNA short and degenerated  
1102 sequences mostly located in single stranded regions, including internal and apical loops.  
1103 Furthermore, we showed that CspA stimulates the translation at low temperature from its  
1104 37°C-form mRNA, which adopts a large and irregular hairpin structure sequestering the  
1105 SD sequence (Fig. 7). This CspA-dependent translational stimulation is observed with  
1106 other mRNAs. In all tested mRNAs, with the exception of *cspD*, we identified a cross-link  
1107 positioned between 9-12 nts from the initiation triplet. We propose that this region of  
1108 mRNAs could be a preferential CspA binding site since it is usually poorly structured (Del  
1109 Campo, 2015). In spite of this interaction, our results demonstrate that CspA enhances the  
1110 translation of only some of the mRNAs that it is able to bind. Our functional experiments  
1111 performed with *cspA* mRNA demonstrate that the translational stimulation affects  
1112 elongation rather than initiation. Particularly, the RelE-walking experiment proves that this  
1113 activity consists in facilitating ribosome progression on the mRNA at low temperature.

1114           During translation the ribosome is able to melt secondary structures of the mRNA  
1115 thanks to the helicase activity of S3, S4 and S5 proteins (Qu et al., 2011). It is very likely  
1116 that this activity could be partly impaired by the low temperature, which is known to  
1117 stabilize base pairing interactions, making it harder for the ribosome to melt the secondary  
1118 structures (Liu et al., 2014). The presence of CspA on the mRNA could be useful to  
1119 facilitate ribosome progression either by destabilizing some positions and/or by preventing  
1120 the re-formation of the secondary structures after the first elongating ribosome has  
1121 unwound them.

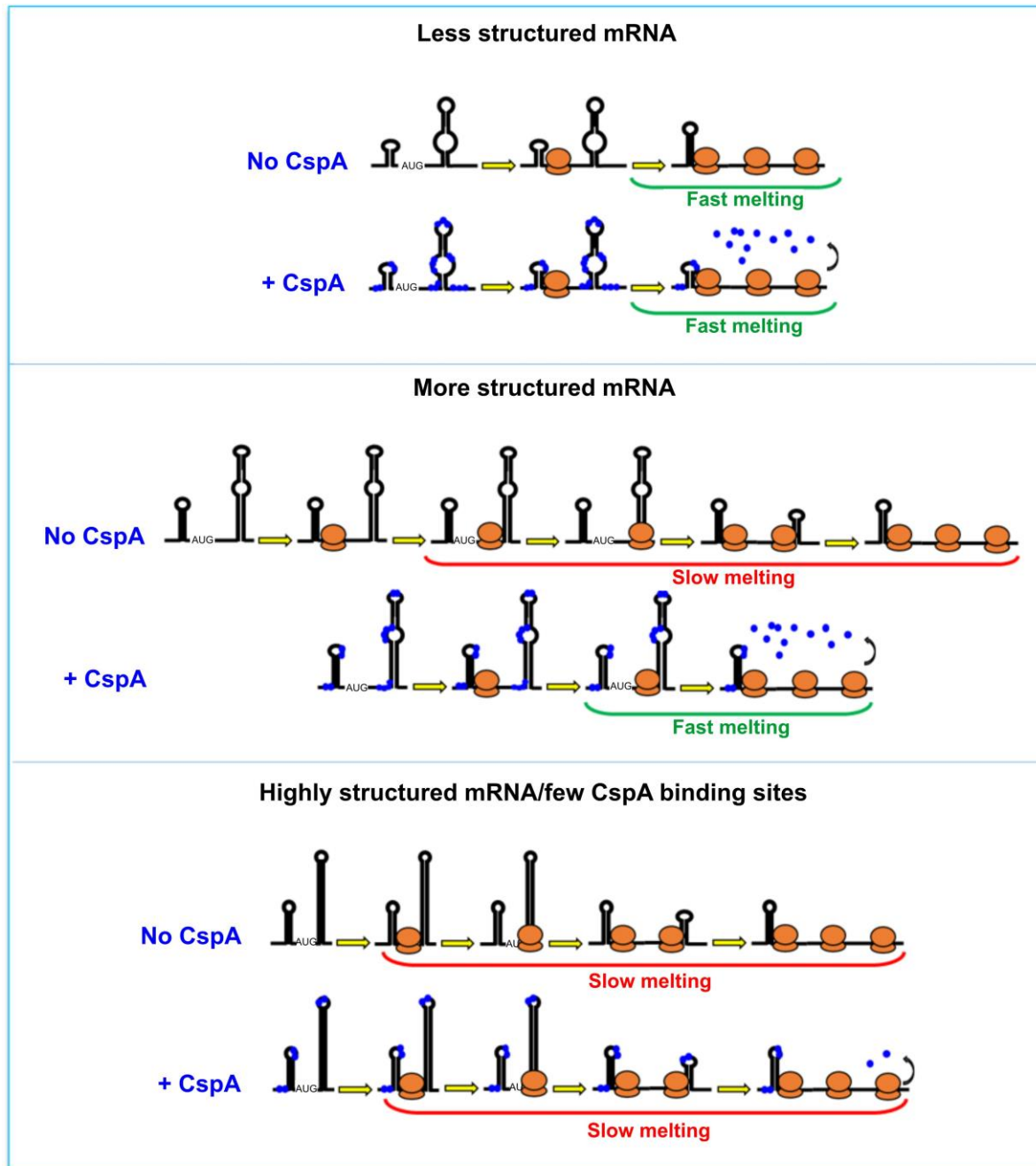
1122           Based on our data, two mechanistic models, not mutually exclusive, can co-exist.  
1123 The first model builds on the CspA RNA chaperone activity (Rennella et al., 2017). This  
1124 model outlines how CspA stimulates annealing of two complementary RNA hairpins by  
1125 weakening the RNA base pairing interactions which prevent the RNA to reach its final and  
1126 less energetic state, to form a thermodynamically more stable hetero-duplex. Therefore, in  
1127 the presence of translating ribosomes, the destabilization of mRNA structures will increase  
1128 the proportion of single-stranded regions thus facilitating ribosome progression. In the  
1129 second model, the amount of the mRNA-bound CspA increases as the translating  
1130 ribosomes open up the mRNA structures. In this case, stimulation during translation would  
1131 not depend on the amount of CspA pre-bound to the mRNA but rather on the capacity of  
1132 CspA to rapidly bind (or re-bind) the regions melted by the passage of the first ribosome  
1133 and keep them single-stranded. This RNA chaperone activity has been dubbed  
1134 “overcrowding” (Cristofari and Darlix, 2002).

1135 Both models would predict an easy displacement of CspA molecules as the ribosomes transit on the mRNA  
1136 interaction sites and can explain the “CspA paradox” (Fig. 11). In fact, ribosome progression  
1137 would be stimulated by CspA only with structured mRNAs whose conformational state is  
1138 stabilized by the low temperature, while the effect will not be seen with mRNAs carrying a  
1139 more open conformation, intrinsically suitable for translation at low temperature. It can thus

1140 be predicted that translation of mRNAs that are too structured and that contain too few  
1141 sites for CspA binding would be little stimulated by CspA.

1142

1143



1180

1181

1182

1183

1184

1185

1186

1187

1188

1189

1190

**FIGURE 11. The CspA paradox.** CspA would ensure ribosome progression by maintaining the bound regions unstructured and/or destabilizing the helices when ribosomes translate along the mRNA. This effect will not be seen with mRNAs attaining an open conformation compatible with translation at low temperature, or in the case of mRNAs that are either structured or containing few sites suitable for CspA binding.



1191

1192 *Stimulation of cspA mRNA translation is one of the first tasks of CspA during cold*

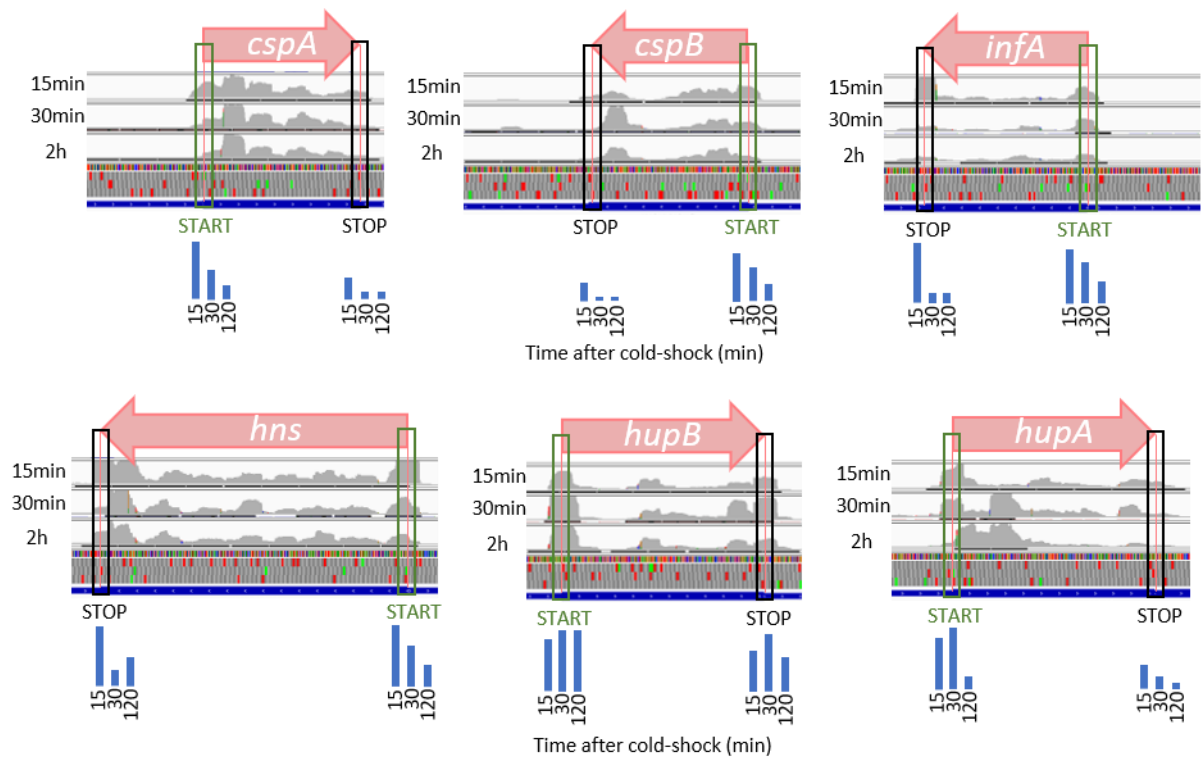
1193 *acclimation*

1194 At the beginning of the acclimation phase, both CspA and its mRNA are already  
1195 present and the translation activation could be rapidly achieved through their interaction.  
1196 Indeed, immediately after the cold stress the *cspA* mRNA transcribed at 37°C is stabilized  
1197 100 times, with its half-life increasing from 12 seconds to 20 minutes (Fang et al., 1997;  
1198 Goldenberg et al., 1996). CspA protein is also known to be abundant at 37°C during early  
1199 exponential growth, when its concentration reaches up to 50 µM (Brandi et al., 1999).  
1200 Under these conditions the cold-shock induction of *cspA* is rather low (only about 3-fold)  
1201 and at the onset of the cold stress the cells use predominantly *cspA* mRNA and CspA  
1202 protein already synthesized at 37°C. Therefore, the capacity of CspA to favor the  
1203 translation of its mRNA folded in the 37°C-conformation in the cold can speed up the  
1204 accumulation of more *cspA* product, in a positive auto-regulatory loop. Our data suggest  
1205 that the translational stimulation by CspA should take place at concentrations  $\geq 25$  µM. In  
1206 addition, probing/footprinting experiments suggested that CspA does not produce  
1207 important conformational changes on the full-length pre-folded *cspA* mRNA, even at  
1208 concentrations  $> 100$  µM. However, CspA seems to affect the conformation of a *cspA*  
1209 mRNA fragment corresponding to the first 87 nts at concentrations  $> 50$  µM. Therefore,  
1210 CspA could play different roles in the cell depending on its expression level. When present  
1211 at concentrations  $< 50$  µM, its main effect would be to favor the progression of the  
1212 ribosome on its and other mRNAs, whereas at higher concentration, CspA could have an  
1213 impact on the co-transcriptional folding process of its targets, *cspA* mRNA *in primis*. This  
1214 hypothesis is supported by the recent work of Zhang and coworkers (2018), which have  
1215 demonstrated that at a concentration of 100 µM, CspA can modulate the structure of its  
1216 mRNA, as well as that of *cspB*, thereby making it more susceptible to degradation at the



1217 end of the acclimation phase. Zhang *et al.* have also shown that CspA contributes to  
1218 support translation recovery of the other genes during cold-shock. This result is in  
1219 agreement with our data, which show that CspA favors the translation of other mRNAs.  
1220 Therefore, we have re-analyzed ribosome profiling data from Zhang *et al.* to understand if  
1221 we could observe *in vivo* the same mechanism of stimulation of translation progression  
1222 from initiation to elongation operated by CspA. Analogously to our *in vitro* ReIE walking  
1223 assay, ribosome profiling experiments allow to map ribosome pausing or stalling sites,  
1224 which are evinced by peaks of ribosome protected fragments. Interestingly, in the cell  
1225 subjected to cold shock the peaks at the initiation codons of the mRNAs tested in this as  
1226 well as in a previous work (Giuliodori et al., 2004) progressively decrease with the  
1227 accumulation of CspA during the acclimation phase (Fig. 12). These data confirm the  
1228 possibility that our proposed model for CspA stimulation of translation could take place *in*  
1229 *vivo* on different mRNAs.

1230 In addition to CspA orthologues present in all bacterial taxa, multiple paralogues  
1231 have wide evolutionary distribution (Graumann and Marahiel, 1996). Some of these  
1232 paralogues carry out overlapping functions, as demonstrated by the fact that in *E. coli* four  
1233 out of nine *csp* genes must be deleted to obtain a cold-sensitive phenotype and that the  
1234 overexpression of any member of the *csp* family (except for *cspD*) suppresses the  
1235 phenotype (Xia et al., 2001). It is also known that these small proteins act as anti-  
1236 termination factors during transcription and can bind both ssDNA and RNA with different  
1237 specificity. CspB, CspC and CspE display specificity for 5'-UUUUU-3', 5'-AGGGAGGGA-  
1238 3' and 5'-AAAUUU-3' sequences, respectively, with  $K_D$  values in the range of 1-10  $\mu$ M,  
1239 similar to that calculated for CspA. Thus, it is conceivable that during cold-shock various  
1240 Csp could be bound to the mRNAs to regulate their transcription or modulate their  
1241 structure, stability and translation, possibly in a concentration-dependent manner as in the  
1242 case of CspA.



1243

1244

1245

1246

1247

1248

1249

1250

1251

1252

1253

1254

1255

1256

1257

1258

1259

1260

1261

1262

1263

1264

1265

**FIGURE 12. *In vivo* analysis of translation progression during cold acclimation.** Ribosome profiling data obtained at 15 minutes, 30 minutes and 2 hours after temperature down-shift (10 °C), have been obtained from GEO series GSE103421 (Zhang et al., 2018). Row data have been trimmed of adapter sequences and bad quality reads, before being aligned on *E. coli* genome (NC\_000913.3). Coverage tracks of aligned reads from ribosome protected fragments indicate the depth of the reads displayed at each locus. To compare different positions of the same region (coding sequence), each track has been normalized on the average of the density peaks of the region, excluding the peaks on the start and stop codons. The blue bars represent the quantization of peak densities at the start and stop codons at the three time points. From left to right, 15 minutes, 30 minutes and 2 hours, respectively. Normalized coverage tracks for *cspA*, *cspB*, *infA* and *hns* mRNAs show peaks on start codons which progressively decrease during cold acclimation. Normalized coverage tracks for *hupA* and *hupB* mRNAs do not show the same trend and their initiation peaks remain quite high even after several minutes of cold acclimation. *CspD* mRNA is not expressed under these conditions.

## 1266 **MATERIALS AND METHODS**

### 1267 **General preparations and buffers**

1268 *Escherichia coli* MRE600 70S ribosomes, S100 post-ribosomal supernatant, 30S  
1269 ribosomal subunits and purified initiation factors IF1, IF2, and IF3 were prepared as  
1270 described previously (Giuliodori et al., 2004; Giuliodori et al., 2007).

1271 The following buffers were used:

1272 *Buffer A*: 25 mM tris-HCl, pH 8.5, 5% glycerol, 100 mM NaCl, 0.025% Nonidet P40; *Buffer*  
1273 *B*: 25 mM tris-HCl, pH 8, 1.3 M NaCl, 5% glycerol, 6 mM  $\beta$ -mercaptoethanol, 0.1 mM  
1274 PMSF, 0.1 mM benzamidine; *Buffer C*: 25 mM tris-HCl, pH 8.0, 700 mM NaCl, 5% glycerol,  
1275 6 mM  $\beta$ -mercapto-ethanol, 0.1 mM PMSF, 0.1 mM benzamidine; *Buffer D*: 25 mM tris-HCl,  
1276 pH 8.0, 300 mM of NaCl, 5% glycerol, 20 mM Imidazole, 6 mM  $\beta$ -mercaptoethanol, 0.1  
1277 mM PMSF, 0.1 mM benzamidine; *Buffer E*: 25 mM tris-HCl, pH 8.0, 300 mM of NaCl, 5%  
1278 glycerol, 300 mM Imidazole, 6 mM  $\beta$ -mercaptoethanol, 0.1 mM PMSF, 0.1 mM  
1279 benzamidine; *Buffer F*: 25 mM tris-HCl, pH 8.0, 100 mM NaCl, 5% glycerol, 6 mM  $\beta$ -  
1280 mercaptoethanol, 0.1 mM PMSF, 0.1 mM benzamidine; *Buffer G*: 25 mM tris-HCl, pH 8.0,  
1281 300 mM NaCl, 5% glycerol, 6 mM  $\beta$ -mercaptoethanol, 0.1 mM PMSF, 0.1 mM  
1282 benzamidine; *Buffer H*: 20 mM tris-HCl, pH 7.1, 10 mM NH<sub>4</sub>Cl, 1 mM MgCl<sub>2</sub>, 10% glycerol,  
1283 0.1 mM EDTA, 6 mM  $\beta$ -mercaptoethanol; *Buffer I*: 20 mM Hepes-KOH, pH 7.5, 10 mM  
1284 MgCl<sub>2</sub>, 50 mM KCl; *Buffer L*: 10 mM Tris-HCl pH 7.5, 60 mM NH<sub>4</sub>Cl, 1 mM DTT, 7 mM  
1285 MgCl<sub>2</sub>; *Buffer M*: 20 mM Tris-HCl pH 7.5, 60 mM KCl, 1 mM DTT, 10 mM MgCl<sub>2</sub>; *Buffer N*:  
1286 20 mM Na-cacodylate, pH 7.2, 10 mM MgCl<sub>2</sub>, 50 mM KCl; *Buffer O*: 20 mM Tris-HCl pH  
1287 7.5, 60 mM KCl, 40 mM NH<sub>4</sub>Cl, 3 mM DTT, 10 mM MgCl<sub>2</sub>, 0.002mg/ml BSA; ITC buffer: 20  
1288 mM Tris-HCl pH 7.1, 10 mM NH<sub>4</sub>Cl, 7 mM MgCl<sub>2</sub>, 10% glycerol, 0.1 mM EDTA, 6 mM  $\beta$ -  
1289 mercaptoethanol.

1290

1291 **Molecular cloning, expression and purification of CspA**

1292 The coding region of *E. coli cspA* gene was amplified by PCR from the pUT7cspA  
1293 construct (Giuliodori et al., 2010) using the forward primer G655 5'-  
1294 CATGCCATGGCCGGTAAAATGACTGGTATCG-3' and the reverse primer G656 5'-  
1295 CGGGATCCTTACAGGCTGGTTACGTTAC-3' and cloned into the pETM11 vector  
1296 (Dümmler et al. 2005) using NcoI and BamHI restriction sites. Because the introduction of  
1297 the NcoI restriction site had changed the second amino acid of the CspA sequence, after  
1298 the molecular cloning the wt sequence was restored by mutagenesis using the  
1299 QuikChange Site-Directed Mutagenesis Kit (Agilent Technologies, Inc., Santa Clara, CA),  
1300 the pETM11-CspA plasmid as DNA template and the mutagenic primers G670 5'-  
1301 TTTCAGGGCGCCATGTCCGGTAAAATGACTG-3' and G671 5'-  
1302 CAGTCATTTTACCGGACATGGCGCCCTGAAA-3'.

1303 Overproduction of protein CspA was induced into a culture of *E. coli* BL21 (DE3)/pLysS  
1304 cells grown in LB medium at 37°C till OD<sub>600</sub> = 0.4 by the addition of 1 mM of isopropylbeta-  
1305 D-1-thiogalactopyranoside (IPTG). After transferring the culture to 20°C for 12 h, cells  
1306 were harvested by centrifugation and the pellet resuspended in Buffer A and stored at -  
1307 80°C. After thawing, cells were diluted in an equal volume of Buffer B and lysed by  
1308 sonication. The resulting cell extract, cleared by centrifugation, was loaded onto a nickel-  
1309 nitrilotriacetic acid (Ni-NTA) chromatographic column equilibrated in Buffer C. After  
1310 washing in Buffer D, protein CspA was eluted using Buffer E, pooled and dialyzed against  
1311 Buffer F. To remove the His-Tag sequence, 15 mg of CspA were incubated for 4 h at 20°C  
1312 with the His-Tag TEV protease (Kapust et al. 2002). At the end of the incubation, the  
1313 concentration of NaCl was increased to 300 mM and the cleaved CspA was loaded onto a  
1314 Ni-NTA column equilibrated in Buffer G. The flow-through, containing CspA with no His-  
1315 Tag, was dialysed overnight at 4°C against Buffer H. Then, CspA was concentrated by

1316 centrifugation in Microcon tubes (Amicon-Millipore) with 3 KDa cut-off at 13.8 krcf, 4°C,  
1317 until the concentration was  $\geq 400 \mu\text{M}$  and stored at -80°C in small aliquots. The purity of  
1318 CspA protein was checked by 18% SDS-PAGE.

1319

### 1320 **mRNA preparation**

1321 The DNA templates used *for in vitro* transcription of the various mRNAs were constructed  
1322 as specified in Giuliadori et al., 2010 and Di Pietro et al., 2013. All mRNAs obtained by *in*  
1323 *vitro* transcription with T7 RNA polymerase were purified and labelled as described in  
1324 Giuliadori et al., 2010.

1325

### 1326 **Translation assays**

1327 Before use, the mRNAs were denatured at 90°C for 1 min in RNase free H<sub>2</sub>O and  
1328 renatured for 15 min at 15°C or 37°C in Buffer I. When required, CspA was added after  
1329 renaturation at the concentrations indicated in the figures.

1330 *In vitro* translation reactions were carried out in 30  $\mu\text{L}$  containing 20 mM Tris-HCl, pH 7.7,  
1331 12 mM Mg acetate, 80 mM NH<sub>4</sub>Cl, 2 mM DTT, 2 mM ATP, 0.4 mM GTP, 10 mM  
1332 phosphoenolpyruvate, 0.025  $\mu\text{g}$  of pyruvate kinase/ $\mu\text{L}$  reaction, 200  $\mu\text{M}$  of each amino  
1333 acid (minus Alanine), 5  $\mu\text{M}$  [<sup>3</sup>H] Alanine (309 mCi/mmol), 50 mM cold Alanine, 0.12 mM  
1334 citrovorum (Serva) and 0.4 U/ $\mu\text{L}$  of RNasin (Promega). The reaction mixture also  
1335 contained 30 pmoles of *in vitro* transcribed mRNAs and either the amount of S30 crude  
1336 extracts corresponding to 20 pmoles of 70S ribosomes or 30 pmoles of purified 70S  
1337 ribosomes, 15 pmoles of purified Initiation Factors IF1, IF2 and IF3, and 2  $\mu\text{L}$  of S100 post-  
1338 ribosomal supernatant. After incubation for the indicated times and temperatures, samples  
1339 (15  $\mu\text{L}$ ) were withdrawn from each reaction mixture and the incorporated radioactivity  
1340 determined by hot-trichloroacetic acid (TCA) method.

1341 Initiation complex (IC) formation assays (filter binding) were carried out in 30  $\mu$ L of Buffer L  
1342 using 0.5  $\mu$ M 30S ribosomal subunits either alone (for the 30S IC) or in the presence of 1  
1343  $\mu$ M of 50S subunits (for the 70S IC), 0.5  $\mu$ M  $^{35}\text{S}$ -fMet-tRNA, 0.5 mM GTP, 0.5  $\mu$ M IF1, 0.5  
1344  $\mu$ M IF2, 0.5  $\mu$ M IF3, 1  $\mu$ M *cspA* and 0.4 U/  $\mu$ L of RNasin (Promega). Binding of  $^{32}\text{P}$ -  
1345 labelled *cspA* mRNA to 30S subunits was performed in 40  $\mu$ l of Buffer L containing 20  
1346 pmoles of *cspA* mRNA and 9000 cpm of [ $^{32}\text{P}$ ] *cspA* mRNA, 0.4 U/ $\mu$ L of RNasin (Promega),  
1347 20 pmoles of 30S subunits and either 30 pmoles of tRNA<sub>i</sub><sup>fMet</sup> or 30 pmoles of fMet-  
1348 tRNA<sub>i</sub><sup>fMet</sup> and 20 pmoles of IF1, IF2 and IF3. After 30 min incubation at 15°C, the amount  
1349 of initiation complex formed was determined either by filtration through 96-multiscreen-  
1350 HTS-HA Millipore plates (mRNA binding) or by nitrocellulose filtration (30S and 70S IC),  
1351 followed by liquid scintillation counting.

1352 The toeprinting assay was performed essentially as described (Fechter, et al, 2009). The  
1353 reaction was carried out in 10  $\mu$ l of Buffer M containing 0.4 U/ $\mu$ L of RNasin (Promega) in  
1354 the presence of 0.02  $\mu$ M *cspA* mRNA, 4  $\mu$ M tRNA<sub>i</sub><sup>fMet</sup>, 50  $\mu$ M each of dNTPs,  $^{32}\text{P}$ -labeled  
1355 oligo *csp2* (5'-CGAACACATCTTTAGAGCCAT-3'), and 0.2  $\mu$ M of *E. coli* 30S subunits. The  
1356 reaction mixtures were incubated for 30 min at 15°C. Primer extension was conducted with  
1357 4 units of Avian Myeloblastosis Virus (AMV) reverse transcriptase (Sigma) for 1 hour at  
1358 15°C. The reaction products were analysed on 8% PAGE-urea gel.

1359

### 1360 **RNA footprinting assays**

1361 Before use, the RNAs were denatured at 90°C for 1 min in RNase- free H<sub>2</sub>O and renatured  
1362 for 15 min at 15°C or 37°C in the buffers used for enzymatic probing or hydroxyl radical  
1363 cleavage experiments.

1364 Enzymatic probing was carried out on  $^{32}\text{P}$ -end-labeled transcripts (50,000 cpm) essentially  
1365 as described earlier (Giuliodori et al., 2010) after incubating the renatured mRNA with the  
1366 amounts of CspA indicated in the figure legends.



1367 Probing by hydroxyl radical cleavage was performed essentially as described (Fabbretti et  
1368 al., 2007). CspA was allowed to bind *cspA* mRNA in 40  $\mu$ L of Buffer N by incubating 10  
1369 pmoles of renatured mRNA with the indicated amounts of protein CspA in the presence of  
1370 0.4 U/ $\mu$ L of RNasin (Promega). After 15 min at 15°C, H<sub>2</sub>O<sub>2</sub> was added (0.15% final  
1371 concentration) and the cleavage started by adding Fe(II)-EDTA (3 mM final concentration).  
1372 Cleavage was allowed to proceed for 15 sec at 15°C before addition of 260  $\mu$ l quenching  
1373 solution containing 0.3 M Na acetate (pH 5.2) in absolute ethanol. The precipitated  
1374 samples were resuspended in H<sub>2</sub>O, extracted with phenol-chloroform and re-precipitated  
1375 with cold 0.3 M Na acetate (pH 5.2) in absolute ethanol. These reaction products,  
1376 resuspended in 3  $\mu$ L of sterile H<sub>2</sub>O, were then subjected to primer extension analysis as  
1377 described earlier (Fabbretti et al. 2016) using *cspA1*, *csp2* and *cspA3* primers (Giuliodori  
1378 et al., 2010).

1379

### 1380 **CspA-RNA cross-linking**

1381 For the CspA-RNA cross-linking experiments, 0.02  $\mu$ M of the <sup>32</sup>P-labeled primers indicated  
1382 in the figure legends were mixed with 0.35  $\mu$ M of the corresponding mRNAs. After a  
1383 denaturation step at 90°C for 1 min, the samples were incubated at either 15°C or 37°C for  
1384 10 min in Buffer I containing 0.4 U/ $\mu$ L of RNasin (Promega). Following renaturation, the  
1385 reaction mixtures were dispensed in tubes containing increasing amounts of purified CspA  
1386 (reaction volumes: 10  $\mu$ L) and the protein was allowed to bind for 10 min at the indicated  
1387 temperatures. Subsequently, the samples were transferred to an ice-cold plate and U.V.  
1388 irradiated for 2 min using the GS Gene-linker BioRad (180 mJ, 254 nm bulbs at 12 cm  
1389 from the U.V. source). The cross-linked RNA was primer-extended using AMV Reverse  
1390 Transcriptase as previously described (Giuliodori et al., 2010).

1391

### 1392 **Isothermal titration calorimetry (ITC)**

1393 All samples were dialyzed against ITC buffer using centrifugal filter units (Centricon, Merck  
1394 Millipore), 3 K for CspA and 100 K for *E. coli* ribosome. ITC experiments were done on the  
1395 microcalorimeter MicroCal PEAQ-ITC (Microcal-Malvern Panalytical, Malvern, UK). For  
1396 CspA/ribosome binding studies, experiments were done by successive injections of CspA  
1397 in 30S, 50S or 70S solution at three different temperatures (15, 25 and 35°C). Data were  
1398 analyzed with MicroCal PEAQ-ITC Analysis Software.

1399

#### 1400 **RelE walking assay**

1401 RelE toxin was expressed and purified as described earlier (Andreev et al. RNA 2008).  
1402 Ribosome progression on *cspA* mRNA was monitored by analysing the amount of RelE  
1403 cleavages obtained by ribosomes paused at different sites on the mRNA. *In vitro*  
1404 translation was carried out in 10  $\mu$ L using the PURExpress kit (NEB) according to the  
1405 commercial protocol in the presence of a mix of  $^{32}$ P-radiolabeled *cspA* mRNA (200000  
1406 cpm/ $\mu$ L) and cold *cspA* mRNA (0.8  $\mu$ M), previously folded at 15°C or 37°C. When present,  
1407 CspA was added at concentration of 30  $\mu$ M. The reaction was incubated 2h at 15°C, and  
1408 blocked by addition of chloramphenicol (1 mM) and different concentration of RelE as in  
1409 figure 2, for 15 min at 15°C. The RNA fragments were then phenol extracted, subjected to  
1410 8% PAGE-urea and revealed by autoradiography. Quantization of each band was done  
1411 using ImageQuant TL (GE Healthcare) and signal normalization was done using the sum  
1412 of the quantization of all the bands present in each lane.

1413

#### 1414 **RNA Electrophoretic mobility shift assay**

1415 Radiolabelled purified *187cspA* RNA (Giuliodori et al., 2010), 50000 cps/sample, at  
1416 concentration < 1  $\mu$ M, was denatured and renatured at 15°C or 37°C, as described  
1417 above. For each experiment, increasing concentrations of purified CspA (30-211  $\mu$ M) were  
1418 added to the 5' end labelled *187cspA* RNA in a total volume of 10  $\mu$ L in Buffer O

1419 containing 0.4 U/ $\mu$ L of RNasin (Promega). Complex formation was performed at 15°C or  
1420 37°C for 15 min. After incubation, 10  $\mu$ L of glycerol blue was added and the samples were  
1421 loaded on a 10% PAGE under non-denaturing conditions (1h, 300 V, 4°C).

1422

### 1423 **Steady-state fluorescence spectroscopy**

1424 To measure binding affinity between CspA and different RNA oligonucleotides, intrinsic  
1425 tryptophan fluorescence quenching experiments with 1  $\mu$ M of CspA and increasing amount  
1426 of RNA oligonucleotides was performed in Buffer H. Fluorescence measurements were  
1427 performed in quartz cells at 20  $\pm$  0.5°C on a Fluoromax-4 fluorimeter (HORIBA Jobin-Yvon  
1428 Inc., NJ., USA). The excitation wavelength was set at 295 nm for selective excitation of  
1429 tryptophan residues and the emission wavelength was scanned from 305 to 450 nm. The  
1430 peak of emission at 351 nm was used to measure the quenching effect. Increasing  
1431 amounts of RNA (from 0.05  $\mu$ M to 18  $\mu$ M as described in figure 6) were added and the  
1432 quartz cell was rapidly homogenized before fluorescence emission measurements.  
1433 Fluorescence intensities were corrected for buffer fluorescence and dilution effects.  
1434 Binding parameters were calculated as described in Dubois et al., 2018.

1435

### 1436 **3D model of CspA-target RNA interaction**

1437 CspA crystal structure (pdb file 1MJC (Schindelin et al., 1994)) was superposed to the  
1438 crystal structure of *B. subtilis* CspB in complex with an eptanucleotide RNA oligo  
1439 (GUCUUUA) (pdb file 3PF4 Sachs et al., 2012). Oligo 1 (AACUGGUA) sequence was then  
1440 modelled on the RNA structure by Assemble2 software (Jossinet et al., 2010).

1441

1442

### 1443 **ACKNOWLEDGEMENTS**

1444 We thank Claudio Gualerzi, Pascale Romby and Serena Bernacchi for critical reading of  
1445 the manuscript and helpful discussions. We thank Benoît Meyer for the help in the ITC  
1446 experiments.

1447

## 1448 **Funding**

1449 The work was supported by the “Projet International de Coopération Scientifique” (PICS)  
1450 No. PICS 5286 between France and Italy to [S.M.]. This work was supported and  
1451 published under the framework of the LABEX: ANR-10-LABX-0036 NETRNA as part of the  
1452 investments for the future program and of ANR-17-EURE-0023 to [P.R.] from the French  
1453 National Research Agency.

1454

## 1455 **Author contributions**

1456 Conceptualization, A.M.G. and S.M.; Methodology, A.M.G and S.M; Investigation, A.M.G.,  
1457 M. D., R. B., R. G., E. S. and E. E.; Writing – Original Draft, A.M.G. and S.M.; Writing –  
1458 Review & Editing, A.M.G., M. D., R. B., R. G., E. S., V. H., E.E. and S.M; Visualization,  
1459 A.M.G.; Supervision, A.M.G., E.E. and S.M.; Resources, A.M.G., E.E. and S.M.

1460

## 1461 **Competing interests**

1462 The authors declare no competing interests.

1463

1464

1465

## 1466 **REFERENCES**

1467 Andreev, D., Hauryliuk, V., Terenin, I., Dmitriev, S., Ehrenberg, M., Shatsky, I. (2008). The  
1468 bacterial toxin RelE induces specific mRNA cleavage in the A site of the eukaryote  
1469 ribosome. *RNA* 14, 233-239.

1470

- 1471 Bae, W., Phadtare, S., Severinov, K., and Inouye, M. (1999). Characterization of  
1472 *Escherichia coli* cspE, whose product negatively regulates transcription of cspA, the gene  
1473 for the major cold shock protein. *Molecular microbiology* 31, 1429-1441.  
1474
- 1475 Barria, C., Malecki, M., and Arraiano, C.M. (2013). Bacterial adaptation to cold.  
1476 *Microbiology* 159, 2437–2443.  
1477
- 1478 Brandi, A., Pietroni, P., Gualerzi, C.O., and Pon, C.L. (1996). Post-transcriptional  
1479 regulation of CspA expression in *Escherichia coli*. *Mol. Microbiol.* 19, 231–240.  
1480
- 1481 Brandi, A., Spurio, R., Gualerzi, C.O., and Pon, C.L. (1999). Massive presence of the  
1482 *Escherichia coli* “major cold-shock protein” CspA under non-stress conditions. *EMBO J.* 18,  
1483 1653–1659.  
1484
- 1485 Brandi, A., Giangrossi, M., Giuliadori, A.M., and Falconi, M. (2016) An Interplay among FIS,  
1486 H-NS, and Guanosine Tetraphosphate Modulates Transcription of the *Escherichia*  
1487 *coli* cspA Gene under Physiological Growth Conditions. *Front. Mol. Biosci.* 24, 3-19.  
1488
- 1489 Broeze, R.J., Solomon, C.J., and Pope, D.H. (1978). Effects of low temperature on in vivo  
1490 and in vitro protein synthesis in *Escherichia coli* and *Pseudomonas fluorescens*. *J*  
1491 *Bacteriol.* 134, 861–874.  
1492
- 1493 Cristofari, G., and Darlix, J.L. (2002). The ubiquitous nature of RNA chaperone proteins.  
1494 *Progress in Nucleic Acid Research and Molecular Biology* 72, 223-268.  
1495
- 1496 Crooks, G.E., Hon, G., Chandonia, J.M., Brenner, S.E. (2004). WebLogo: A sequence logo  
1497 generator, *Genome Research*, 14, 1188-1190.  
1498
- 1499 Del Campo, C., Bartholomäus, A., Fedyunin, I., and Ignatova, Z. (2015). Secondary  
1500 structure across the bacterial transcriptome reveals versatile roles in mRNA regulation and  
1501 function. *PLoS Genet.*, 11: e1005613.  
1502
- 1503 Di Pietro, F., Brandi, A, Dzeladini, N., Fabbretti, A., Carzaniga, T., Piersimoni, L.,  
1504 Pon, C.L., and Giuliadori, A.M. (2013) Role of the ribosome-associated protein PY in the  
1505 cold-shock response of *Escherichia coli*. *Microbiologyopen.* 2, 293-307.  
1506
- 1507 Donis-Keller, H., Maxam, A.M., and Gilbert, W. (1977). Mapping adenines, guanines, and  
1508 pyrimidines in RNA. *Nucleic Acids Res.* 4, 2527–2538.  
1509
- 1510 Dubois, N., Khoo, K.K, Ghossein, S., Seissler, T., Wolff, P., McKinstry, W.J., Mak, J.,  
1511 Paillart, J.C., Marquet, R. and Bernacchi, S. (2018) The C-terminal p6 domain of the HIV-1  
1512 Pr55Gag precursor is required for specific binding to the genomic RNA. *RNA Biol.* 15, 923-  
1513 936.  
1514
- 1515 Dümmler, A., Lawrence, A.M., and De Marco, A. (2005). Simplified screening for the  
1516 detection of soluble fusion constructs expressed in *E. coli* using a modular set of vectors.  
1517 *Microb. Cell Fact.* 4, 34.  
1518
- 1519 Duval, M., Marenna, A., Chevalier, C., Marzi, S. (2017). Site-Directed Chemical Probing to  
1520 map transient RNA/protein interactions. *Methods.* 117, 48-58.  
1521

- 1522 Ermolenko, D.N., and Makhatadze, G.I. (2002). Bacterial cold-shock proteins. *Cell Mol Life*  
1523 *Sci* 59, 1902-1913.  
1524
- 1525 Etchegaray, J.P., and Inouye, M. (1999). A sequence downstream of the initiation codon is  
1526 essential for cold shock induction of *cspB* of *Escherichia coli*. *J Bacteriol.* 181, 5852–5854.  
1527
- 1528 Fabbretti, A., Milon, P., Giuliadori, A.M., Gualerzi, C.O., and Pon, C.L. (2007) Real-time  
1529 dynamics of ribosome-ligand interaction by time-resolved chemical probing methods.  
1530 *Methods Enzymol.* 430, 45-58.  
1531
- 1532 Fabbretti, A., Schedlbauer, A., Brandi, L., Kaminishi, T., Giuliadori, A.M., Garofalo, R.,  
1533 Ochoa-Lizarralde, B., Takemoto, C., Yokoyama, S., Connell, S.R., Gualerzi, C.O., and  
1534 Fucini, P. (2016). Inhibition of translation initiation complex formation by GE81112  
1535 unravels a 16S rRNA structural switch involved in P-site decoding. *Proc. Natl. Acad. Sci.*  
1536 *USA.* 113: E2286-95.  
1537
- 1538 Farewell, A., and Neidhardt, F.C. (1998). Effect of temperature on *in vivo* protein synthetic  
1539 capacity in *Escherichia coli*. *J Bacteriol.* 180, 4704–4710.  
1540
- 1541 Fang, L., Jiang, W., Bae, W., and Inouye, M. (1997). Promoter-independent cold-shock  
1542 induction of *cspA* and its derepression at 37°C by mRNA stabilization. *Mol. Microbiol.* 23,  
1543 355–364.  
1544
- 1545 Fechter, P., Chevalier, C., Yusupova, G., Yusupov, M., Romby, P., and Marzi, S. (2009).  
1546 Ribosomal initiation complexes probed by toeprinting and effect of trans-acting  
1547 translational regulators in bacteria. In *Riboswitches, Methods in Molecular Biology*, A.  
1548 Serganov, ed. (Totowa, NJ, USA, HumanaPress), pp 247-64.  
1549
- 1550 Friedman, S.M., and Weinstein, I.B. (1964). Lack of fidelity in the translation of synthetic  
1551 polyribonucleotides. *Proceedings of the National Academy of Sciences USA* 52, 988–996.  
1552
- 1553 Giangrossi, M., Giuliadori, A.M., Gualerzi, C.O., and Pon, C.L. (2002). Selective  
1554 expression of the beta-subunit of nucleoid-associated protein HU during cold shock in  
1555 *Escherichia coli*. *Mol Microbiol.*, 44, 205-16.  
1556
- 1557 Giangrossi, M., Brandi, A., Giuliadori, A.M., Gualerzi, C.O., and Pon, C.L. (2007). Cold-  
1558 shock-induced *de novo* transcription and translation of *infA* and role of IF1 during cold  
1559 adaptation. *Mol. Microbiol.* 64, 807-21.  
1560
- 1561 Giuliadori, A.M., Brandi, A., Gualerzi, C.O., and Pon, C.L. (2004). Preferential translation  
1562 of cold-shock mRNAs during cold adaptation. *RNA* 10, 265–276.  
1563
- 1564 Giuliadori, A.M., Giangrossi, M., Brandi, A., Gualerzi, C.O., and Pon, C.L. (2007). Cold-  
1565 stress-induced *de novo* expression of *infC* and role of IF3 in cold-shock translational bias.  
1566 *RNA* 13, 1355–1365.  
1567
- 1568 Giuliadori, A.M., Di Pietro, F., Marzi, S., Masquida, B., Wagner, R., Romby, P., Gualerzi,  
1569 C.O., and Pon, C.L. (2010) The *cspA* mRNA is a thermosensor that modulates translation  
1570 of the cold-shock protein CspA. *Mol Cell.* 37, 21-33.  
1571



- 1572 Giuliadori, A. M. (2016). Cold-shock response in *Escherichia coli*: a model system to study  
1573 post-transcriptional regulation. In *Stress and Environmental Regulation of Gene*  
1574 *Expression and Adaptation in Bacteria*. Frans J. de Bruijn Ed. (New Jersey, USA: Wiley-  
1575 Blackwell), pp 859-872  
1576
- 1577 Giuliadori, A.M., Fabbretti, A., and Gualerzi, C. (2019) Cold-Responsive Regions of  
1578 Paradigm Cold-Shock and Non-Cold-Shock mRNAs Responsible for Cold Shock  
1579 Translational Bias. *Int J Mol Sci.* 20. pii: E457.  
1580
- 1581 Goldenberg, D., Azar, I., and Oppenheim, A. B. (1996). Differential mRNA stability of the  
1582 *cspA* gene in the cold-shock response of *Escherichia coli*. *Mol. Microbiol.* 19, 241–248.  
1583
- 1584 Goldenberg, D., Azar, I., Oppenheim, A. B., Brandi, A., Pon, C. L., and Gualerzi, C. O.  
1585 (1997). Role of *Escherichia coli cspA* promoter sequences and adaptation of translational  
1586 apparatus in the cold-shock response. *Mol. Gen. Genet.* 256, 282–290.  
1587
- 1588 Goldstein, J.N., Pollitt, S. and Inouye, M. (1990). Major cold shock protein of *Escherichia*  
1589 *coli*. *Proc. Nati. Acad. Sci. USA* 87, 283-287.  
1590
- 1591 Graumann, P., and Marahiel, M.A. (1996) Some like it cold: response of microorganisms to  
1592 cold shock. *Arch Microbiol*, 166, 293-300.  
1593
- 1594 Graumann, P.L., and Marahiel, M.A. (1998). A superfamily of proteins that contain the  
1595 cold-shock domain. *Trends Biochem. Sci.* 23, 286-90.  
1596
- 1597 Gualerzi, C.O., Giuliadori, A.M., and Pon, C.L. (2003). Transcriptional and post-  
1598 transcriptional control of cold-shock genes. *J. Mol. Biol.* 331, 527–539.  
1599
- 1600 Gualerzi, C.O., Giuliadori, A.M., Brandi, A., Di Pietro, F., Piersimoni, L., Fabbretti, A.,  
1601 and Pon, L. C. (2011). Translation initiation at the root of the cold-shock translational  
1602 bias. In: Rodnina M.V., Wintermeyer W., Green R. (eds) *Ribosomes*. Springer, Vienna.  
1603
- 1604 Hartz, D., McPheeters, D.S., Traut R., and Gold L. (1988). Extension inhibition analysis of  
1605 translation initiation complexes. *Methods Enzymol.* 164, 419-25.  
1606
- 1607 Jiang, W., Hou, Y., and Inouye, M. (1997). CspA, the major cold-shock protein of  
1608 *Escherichia coli*, is an RNA chaperone. *J. Biol. Chem.* 272,196–202.  
1609
- 1610 Jones, P.G., Krah, R., Tafuri, S.R., and Wolffe, A.P. (1992). DNA gyrase, CS7.4, and the  
1611 cold shock response in *Escherichia coli*. *J Bacteriol.* 174, 5798–5802.  
1612
- 1613 Jossinet, F., Ludwig, T.E., and Westhof, E. (2010). Assemble: an interactive graphical tool  
1614 to analyze and build RNA architectures at the 2D and 3D levels. *Bioinformatics* 26, 2057-  
1615 2059.  
1616
- 1617 Kapust, R. B., Tözsér, J., Copeland, T.D., and Waugh, D.S. (2002) The P1' specificity of  
1618 tobacco etch virus protease. *Biochem. Biophys. Res. Commun.* 5, 949–955.  
1619
- 1620 Kremer, W., Schuler, B., Harrieder, S., Geyer, M., Gronwald, W., Welker, C., Jaenicke, R.,  
1621 and Kalbitzer, H.R. (2001). Solution NMR structure of the cold-shock protein from the  
1622 hyperthermophilic bacterium *Thermotoga maritima*. *Eur. J. Biochem.* 268, 2527-2539.

1623

1624 Liu, T., Kaplan, A., Alexander, L., Yan, S., Wen, J.D., Lancaster, L., Wickersham, C.E.,  
1625 Fredrick, K., Noller, H., Tinoco, I., *et al.* (2014). Direct measurement of the mechanical  
1626 work during translocation by the ribosome. *eLife* 3, e03406.

1627

1628 La Teana, A., Brandi, A., Falconi, M., Spurio, R., Pon, C. L., and Gualerzi, C. O. (1991).  
1629 Identification of a cold shock transcriptional enhancer of the *Escherichia coli* gene  
1630 encoding nucleoid protein H-NS. *Proc. Natl Acad. Sci. USA*, 88, 10907–10911.

1631

1632 Lopez, M.M., and Makhatadze, G.I. (2000). Major cold shock proteins, CspA from  
1633 *Escherichia coli* and CspB from *Bacillus subtilis*, interact differently with single-stranded  
1634 DNA templates. *Biochim Biophys Acta*, 1479, 196-202.

1635

1636 Mayer, O., Rajkowitsch, L., Lorenz, C., Konrat, R., and Schroeder, R. (2007). RNA  
1637 chaperone activity and RNA-binding properties of the *E. coli* protein StpA. *Nucleic Acids*  
1638 *Res.* 35, 1257-1269.

1639

1640 Mitta, M., Fang, L., and Inouye, M. (1997). Deletion analysis of *cspA* of *Escherichia coli*:  
1641 requirement of the AT-rich UP element for *cspA* transcription and the downstream box in  
1642 the coding region for its cold shock induction. *Mol Microbiol* 26, 321–335.

1643

1644 Mueller, U., Perl, D., Schmid, F.X., and Heinemann, U. (2000). Thermal stability and  
1645 atomic-resolution crystal structure of the *Bacillus caldolyticus* cold shock protein. *J. Mol.*  
1646 *Biol.* 297, 975-988.

1647

1648 Newkirk, K., Feng, W., Jiang, W., Tejero, R., Emerson, S.D., Inouye, M., and Montelione,  
1649 G.T. (1994). Solution NMR structure of the major cold shock protein (CspA) from  
1650 *Escherichia coli*: identification of a binding epitope for DNA. *Proc. Natl Acad. Sci. USA* 91,  
1651 5114-5118.

1652

1653 Neubauer, C., Gao, Y-G., Andersen, K.R., Dunham, C.M., Kelley, A.C., Hentschel, J.,  
1654 Gerdes, K., Ramakrishnan, V., Brodersen, D.E. (2009). The Structural Basis for mRNA  
1655 Recognition and Cleavage by the Ribosome-Dependent Endonuclease RelE. *Cell.* 139,  
1656 1084–1095.

1657

1658 Pedersen, K., Zavialov, A.V., Pavlov, M.Y., Elf, J., Gerdes, K., Ehrenberg, M. (2003). The  
1659 bacterial toxin RelE displays codon-specific cleavage of mRNAs in the ribosomal A site.  
1660 *Cell.* 112, 131-140.

1661

1662 Phadtare, S., and Inouye, M. (1999). Sequence-selective interactions with RNA by CspB,  
1663 CspC and CspE, members of the CspA family of *Escherichia coli*. *Mol Microbiol* 33, 1004–  
1664 1014.

1665

1666 Phadtare, S., and Inouye, M. (2004). Genome-wide transcriptional analysis of the cold  
1667 shock response in wild-type and cold-sensitive, quadruple-csp-deletion strains of  
1668 *Escherichia coli*. *J Bacteriol.* 186, 7007-7014.

1669

1670 Phadtare, S. (2004). Recent developments in bacterial cold-shock response. *Curr. Issues*  
1671 *Mol. Biol.* 6, 125-36.

1672

- 1673 Phadtare, S., and Severinov, K. (2009) Comparative analysis of changes in gene  
1674 expression due to RNA melting activities of translation initiation factor IF1 and a cold shock  
1675 protein of the CspA family. *Genes Cells*. *14*, 1227-39.  
1676
- 1677 Qu, X., Wen, J.D., Lancaster, L., Noller, H.F., Bustamante, C., and Tinoco, I., Jr. (2011).  
1678 The ribosome uses two active mechanisms to unwind messenger RNA during translation.  
1679 *Nature* *475*, 118-121.  
1680
- 1681 Rajkowitsch, L., and Schroeder R. (2007). Dissecting RNA chaperone activity. *RNA* *13*,  
1682 2053-60.  
1683
- 1684 Rennella, E., Sara, T., Juen, M., Wunderlich, C., Imbert, L., Solyom, Z., Favier, A., Ayala,  
1685 I., Weinhaupl, K., Schanda, P., *et al.* (2017). RNA binding and chaperone activity of the *E.*  
1686 *coli* cold-shock protein CspA. *Nucleic Acids Res.* *45*, 4255-4268.  
1687
- 1688 Sachs, R., Max, K.E., Heinemann, U., Balbach, J. (2012). RNA single strands bind to a  
1689 conserved surface of the major cold shock protein in crystals and solution. *RNA*, *18*, 65-76.  
1690
- 1691 Serganov, A., Rak, A., Garber, M., Reinbolt, J., Ehresmann, B., Ehresmann, C., Grunberg-  
1692 Manago, M., and Portier, C. (1997). Ribosomal protein S15 from *Thermus thermophilus*-  
1693 cloning, sequencing, overexpression of the gene and RNA-binding properties of the  
1694 protein. *Eur. J. Biochem.* *246*, 291-300.  
1695
- 1696 Shimizu, Y., Inoue, A., Tomari, Y., Suzuki, T., Yokogawa, T., Nishikawa, K., and Ueda, T.  
1697 (2001). Cell-free translation reconstituted with purified components. *Nat. Biotechnol.* *19*,  
1698 751-755.  
1699
- 1700 Schindelin, H., Jiang, W., Inouye, M., and Heinemann, U. (1994). Crystal structure of CspA,  
1701 the major cold shock protein of *Escherichia coli*. *Proc. Natl Acad. Sci. USA* , *91*, 5119-  
1702 5123.  
1703
- 1704 Schnuchel, A., Wiltscheck, R., Czisch, M., Herrler, M., Willimsky, G., Graumann, P.,  
1705 Marahiel, M.A., and Holak, T.A. (1993). Structure in solution of the major cold-shock  
1706 protein from *Bacillus subtilis*. *Nature* *364*, 169-171.  
1707
- 1708 Weber, M.H., and Marahiel, M.A. (2003) Bacterial cold shock responses. *Sci. Prog.*, *86*, 9-  
1709 75.  
1710
- 1711 Withman, B., Gunasekera, T.S., Beesetty, P., Agans, R. and Paliy, O. (2013)  
1712 Transcriptional responses of uropathogenic *Escherichia coli* to increased environmental  
1713 osmolality caused by salt or urea. *Infect Immun.*, *81*, 80-89.  
1714
- 1715 Wolffe, A.P., Tafuri, S., Ranjan, M., and Familiari, M. (1992). The Y-box factors: a family of  
1716 nucleic acid binding proteins conserved from *Escherichia coli* to man. *New Biol.* *4*, 290-298.  
1717
- 1718 Yamanaka, K., and Inouye, M. (1997). Growth-phase-dependent expression of *cspD*,  
1719 encoding a member of the CspA family in *Escherichia coli*. *J Bacteriol.*, *179*, 5126-5130.  
1720
- 1721 Yamanaka, K., Fang, L., and Inouye, M. (1998) The CspA family in *Escherichia coli*:  
1722 multiple gene duplication for stress adaptation. *Mol. Microbiol.*, *27*, 247-255.  
1723

- 1724 Yamanaka, K., Mitta, M., and Inouye, M. (1999). Mutation analysis of the 5'-untranslated  
1725 region of the cold shock *cspA* mRNA of *Escherichia coli*. *J Bacteriol.* *181*, 6284–6291.  
1726
- 1727 Xia, B., Ke, H., and Inouye, M. (2001). Acquirement of cold-sensitivity by quadruple  
1728 deletion of the *cspA* family and its suppression by PNPase S1 domain in *Escherichia coli*.  
1729 *Mol Microbiol*, *40*, 179– 188.  
1730
- 1731 Zhang, Y., Burkhardt, D.H., Rouskin, S., Li, G.W., Weissman, J.S., and Gross C.A. (2018).  
1732 A Stress Response that Monitors and Regulates mRNA Structure Is Central to Cold Shock  
1733 Adaptation. *Mol Cell*, *70*, 274-286  
1734
- 1735 Zuker, M. (2003). Mfold web server for nucleic acid folding and hybridization prediction.  
1736 *Nucleic Acids Res.* *31*, 3406-15.  
1737
- 1738 patent US7118883b2) , registrato 23 ottobre 2001, Inoue, Ueda.  
1739